Since hantaviruses are intimately associated with specific rodent hosts with which they are believed to have coevolved, the distribution of human disease generally mirrors that of rodent hosts. Rodent species that are known to carry HPS-causing hantaviruses in North America include, among others, *P. maniculatus* (Sin Nombre virus; SNV) (Childs et al., 1994), *Peromyscus leucopus* (New York virus; NYV) (Song et al., 1994), *Sigmodon hispidus* (Black Creek Canal virus; BCCV) (Rollin et al., 1995), *Oryzomys palustris* (Bayou virus; BAYV) (Morzunov et al., 1995), and *Oligoryzomys couesi* (Catacamas virus; CATV) (Milazzo et al., 2006). Rodents in South America known to carry hantaviruses that are pathogenic to humans include *Oligoryzomys longicaudatus* (Andes virus; ANDV) (Levis et al., 1998), *Calomys laucha* (Laguna Negra virus; LANV) (Johnson et al., 1997), *Oligoryzomys flavescens* (Lechiguanas virus; LECV) (Levis et al., 1998), and many others (Jonsson et al., 2010). Compared to other regions of the world, the hantaviruses of South America tend to be carried by different rodent species at the same time that those rodents carry other viruses, exhibiting a more complex virus–host relationship (Chu et al., 2008; Milazzo et al., 2006; Padula et al., 2004). Thus, information regarding hantaviruses and their hosts suggests that a vast number of rodent species are potential reservoirs for hantaviruses (Jonsson et al., 2010).

In Mexico in particular, none of the hantaviruses identified so far have been associated with cases of HPS. Hantavirus-related studies conducted in Mexico have identified numerous rodents as carriers of hantaviruses. However, the true extent of the diversity of potential rodent reservoirs is not yet known. For example, Playa de Oro virus (OROV), hosted by *Oryzomys couesi*, was identified in Colima in Southwestern Mexico (Chu et al., 2008), and EL Moro Canyon virus (ELMCV) was detected in *R. megalotis* (Rowe et al., 1995). Rodents for which only serological evidence of hantavirus infection is reported include *Reithrodontomys mexicanus* (Hjelle et al., 1995), *Reithrodontomys sumichrasti* (Suzan et al., 2001), *Peromyscus levipes* (Castro-Arellano et al., 2009), *Peromyscus hylocetes*, and *Peromyscus melanotis* (Mantooth et al., 2001).

In our recent epidemiological survey conducted in Mexico in 2006, we identified three distinct hantaviruses circulating in Mexican wild rodents, and these hantaviruses were designated Montano virus (MTNV), Huitzilac virus (HUIV), and Carrizal virus (CARV) (Kariwa et al., 2012). Therefore, a need existed for a thorough epidemiological investigation for the purposes of gaining greater insight into the extent of genetic diversity of Mexican hantaviruses and their relationships to host species. For this purpose an additional 200 rodents were collected (May 2007) and all the specimens ($n = 410$) were examined. The analysis of viral genes and rodent mitochondrial DNA (mtDNA) cytochrome *b* (cyt*b*) genes could reveal the maintenance and transmission patterns of hantaviruses in rodents, thus leading to a broader understanding of the virus–host interaction. Here, we present findings indicating that *P. beatae* is the principal carrier of MTNV while *R. sumichrasti* is the host of CARV.

Wild rodents were captured in May 2006 ($n = 210$) (Kariwa et al., 2012) and May 2007 ($n = 200$) for a survey of hantavirus infection at various locations in Morelos ($n = 72$) and Guerrero ($n = 338$), Mexico. Rodents were trapped and collected from two areas in Morelos (Tres Marias and Zacatepec) and six areas in Guerrero (Fig. 1 and Table 1). Measurements of body weight, sex, total body length, tail length, and hind foot-pad length of the rodents were made and recorded for subsequent identification of rodent species. Blood was collected by cardiac puncture under anesthesia and serum was isolated. Lung, kidney, spleen, heart, and liver tissues were collected and preserved at −80 °C prior to processing.

A Sin Nombre virus (SNV) construct encoding the N protein, kindly supplied by Dr. C.J. Peters (University of Texas, Galveston, TX, USA) was used for the preparation of antigen for screening rodent sera for hantavirus antibodies by enzyme-linked immunosorbent assay (ELISA), as earlier described (Kariwa et al., 2012). The S segment gene of the newly identified Mexican Montano virus (MTNV) was similarly amplified and cloned into a pET43.1b (+) vector (Novagen; EMD Chemicals, Darmstadt, Germany) to generate an N terminal NuSA-fused N protein. Rodent sera were screened for hantavirus antibodies by ELISA and Western blotting (WB) assays using the N protein of SNV or MTNV.

Total RNA from rodent lungs was extracted using the Isogen kit (Nippon Gene, Tokyo, Japan) according to the manufacturer's protocol. Rodent mtDNA from liver tissue was extracted using the mtDNA Extraction CT Kit (Wako Pure Chemicals, Osaka, Japan) according to the manufacturer's protocol. The cyt*b* gene of mtDNA was amplified using the following primers: forward, 5′-CGAAGCTTGATATGAAAAACCATCGTTG-3′ and reverse, 5′-CTGGTTTACAAGACCAGAGTAAT-3′ (Kang et al., 2009). The nucleotide sequences of the amplified virus S genome and rodent mtDNA cyt*b* gene were determined by using the BigDye Terminator v3.1 cycle sequencing kit (Applied Biosystems, Foster City, CA, USA) according to manufacturer's protocol.

The nucleotide sequences of the viral S segment open reading frame (ORF) and the rodent mtDNA cyt*b* genes were aligned using ATGC and Genetyx ver 8.0.0 (Genetics Corp, Tokyo, Japan) computer software. Nucleotide sequence alignment and phylogenetic analysis was conducted using MEGA 4 software (Tamura et al., 2007). The evolutionary relationship between virus and host was inferred using the neighbor-joining method (Saitou and Nei, 1987). The percentage of replicate trees in which the associated taxa clustered together in the bootstrap test (1000 replicates) was calculated (Felsenstein, 1985). The tree was drawn to scale, with branch lengths in the same units as those of the evolutionary distances used to infer the phylogenetic tree. The evolutionary distances were computed using the Maximum Composite Likelihood method (Tamura et al., 2004) and are presented in the units of the number of base substitutions per site.

We carried out an epidemiological survey in the Mexican states of Morelos and Guerrero. From the two surveys, 410 individual rodents were trapped in Morelos (72/410; 17.6%) and Guerrero (338/410; 82.4%) (Table 2). Infected rodents were detected at three of the eight collecting areas surveyed (Tres Marías, Carrizal de Bravo, and Chilpancingo), with an overall hantavirus seroprevalence of 10.5%. Carrizal de Bravo had both the highest number of rodents captured (200/410; 48.8%) and the highest hantavirus seroprevalence (40/200; 20.0%). The genera *Peromyscus* and *Reithrodontomys* were predominant among the several rodent species captured (Table 3). Species-specific seroprevalence was as follows: *P. beatae* (24.4%), *R. sumichrasti* (40%), *P. aztecus evides* (100%), *P. megalops* (2.4%), *R. megalotis* (8%), *M. thomasi* (11.1%), and *N. picta* (16.7%) (Table 3).

For genetic confirmation of rodent species identity, the cyt*b* gene from the 41 hantavirus-positive rodents (as determined by the presence of antibody and/or virus RNA) was amplified, and the nucleotide sequences were determined (Table 4). A database search of the rodent cyt*b* gene and morphological analysis of individual rodents revealed that hantavirus-positive rodents included *P. beatae* (29/41), *R. sumichrasti* (6/41), *P. aztecus evides* (1/41), *P. megalops* (1/41), *R. megalotis* (2/41), *M. thomasi* (1/41), and *N. picta* (1/41).

An examination of lung specimens for the presence of the hantavirus S segment by reverse transcription (RT)-PCR detected RNA in 9.5% (39/410) of individuals, of which 94.9% (37/39) were also seropositive for hantavirus (Table 4). Both hantavirus-specific antibodies and virus genome were detected in the majority of *P. beatae* and *R. sumichrasti* rodents. The entire S segment ORF was successfully amplified from 30/39 hantavirus RNA-positive rodents. The

Table 1
Rodent collection areas in Morelos and Guerrero states.

State, municipality, locality	Topography	Climate	Temp (°C)	Rainfall (mm)	Vegetation
Morelos, Huitzilac					
1a. Tres Marías, Preparatoria Comunitaria, 2852 m asl (above sea level) 19°03′33.8″N, 99°14′58.9″W	Steep volcanic soil	Tempered sub-humid	12.2	1200–1500	Pine, oak, cedar grasses
1b. Tres Marías, Cerro del Tezontle, 2870 m asl, 19°03′15.3″N, 19°15′13.1″W					
Morelos, Zacatepec					
2a. Campo experimental INIFAP, 608 m asl, 18°39′17.3″N, 99°12′08.8″W	Flat, livestock grazing	Sub-humid	24.3	892	Sugar cane, dry forest, thorn forest
2b. Cerro de La Tortuga, 980 m asl, 18°40′19.7″N, 99°12′47.2″W					
Guerrero, Iguala de La Independencia					
3a. Cerro de Tuxpan,5 km N Tuxpan, 1560 m asl, 18°23′36″N, 99°28′36″W	Slightly rough	Sub-humid	22–26	900–1100	Oak forest (3a) tropical dry forest (3b), scrub hawthorn (3c, 3d)
3b. Platanillo, 5.5 km NW Tuxpan, 1050 m asl, 18°23′56″N, 99°29′47″W					
3c. Tuxpan, 2 km E, 970 m asl, 18°21′03″N, 99°27′35″W					
3d. Tuxpan, 1.5 km E, 900 m asl, 18°20′58″N, 99°27′56″W					
Guerrero, Huitzuco de Los Figueroa					
4a. Tlaxmalac, 2.5 km SW, 900 m asl, 18°21′9″N, 99°26′08″W	Slightly rough	Sub-humid	22–26	900–1100	Tropical dry forest
4b. Tlaxmalac, 3.5 km SW, 900 m asl, 18°20′55″N, 99°26′22″W					
Guerrero, Eduardo Neri					
5a. Xochipala, 7.5 km SW, 1740 m asl, 17°46′32″N, 99°42′16″W	Rough	Semi-warm, sub-humid	18–22	900–1100	Oak forest (5a, 5b), tropical dry forest with columnar cactus (6a, 6b)
5b. Xochipala, 9 km SW, 1930 m asl, 17°45′26″N, 99°42′23″W					
6a. Zumpango del Río, 7.5 km NW, 880 m asl, 17°42′50″N, 99°33′17″W					
6b. Zumpango del Río, 3.5 km SW, 1170 m asl, 17°37′22″N, 99°33′00″W					
Guerrero, Leonardo Bravo					
7a. Carrizal de Bravo, 2.5 km SE, 2400 m asl, 17°36′35″N, 99°49′15″W	Slightly rough	Sub-humid	15–18	>1500	Cloud forest (7a, 7c, 7d, 7e) peach orchard (7b)
7b. Los Cajones, 2 km S Carrizal de Bravo, 2560 m asl, 17°36′13″N, 99°50′9″W					
7c. Las Truchas, 3 km SE Carrizal de Bravo, 2400 m asl, 17°35′54″N, 99°49′39″W					
7d. Carrizal de Bravo, 3 km S, 2700 m asl, 17°35′34″N, 99°50′14″W					
7e. Carrizal de Bravo, 4 km SE, 2700 m asl, 17°35′09″N, 99°49′58″W					
Guerrero, Chilpancingo de Los Bravos					
8a. Barranca La Imagen, 3 km SW Palo Blanco, 1130 m asl, 17°22′58″N, 99°28′50″W	Rugged, deep ravines	Semi-warm, sub-humid	18–22	>1500	Riparian forest
8b. Barranca Manguitos, 1.5 km SW Acahuizotla, 1000 m asl, 17°21′25″N, 99°28′51″W					

Numbers in the table correspond to the locations of survey sites shown in Fig. 1.

Table 2
Number of captured rodents and seroprevalence by municipalitie and location in Morelos and Guerrero.

	State	Municipality	Location	Rodents	Hantavirus positive	(%)
1	Morelos	Huitzilac	Tres Marías	60	2	3.3
2		Zacatepec	Zacatepec	12	0	0.0
		Subtotal		72	2	2.8
3	Guerrero	Iguala de La Independencia	Tuxpan	41	0	0.0
4		Eduardo Neri	Xochipala	12	0	0.0
5		Eduardo Neri	Zumpango del Río	9	0	0.0
6		Huitzuco de Los Figueroa	Tlaxmalac	20	0	0.0
7		Leonardo Bravo	Carrizal de Bravo	200	40	20
8		Chilpancingo	Palo Blanco	56	1	1.8
		Subtotal		338	41	12.1
	Total			410	43	10.5

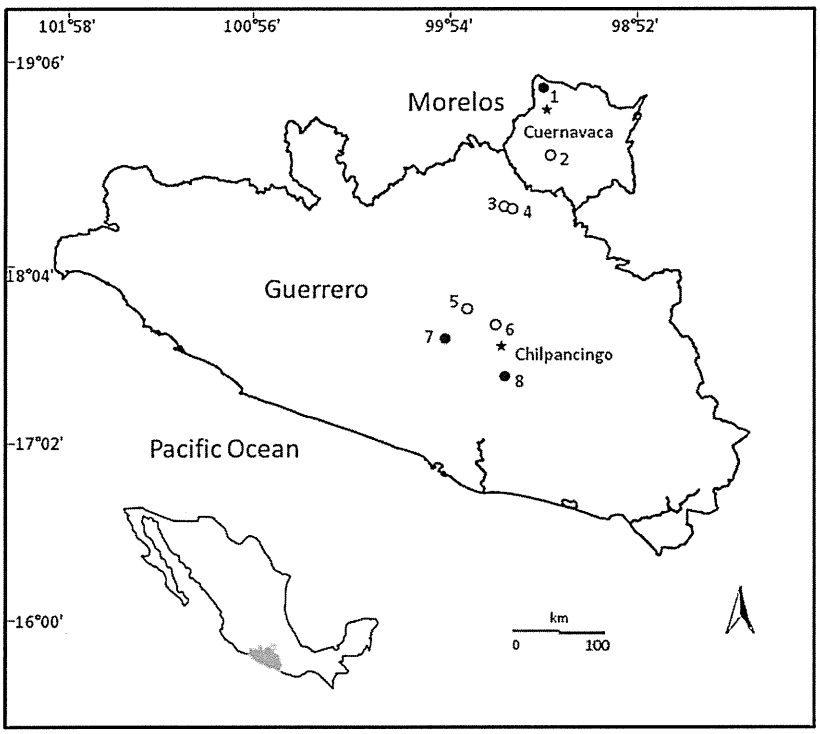

Fig. 1. The sites of wild rodent collection during 2006 and 2007 hantavirus field surveys in Morelos and Guerrero, Mexico. (1) Huitzilac, (2) Zacatepec, in Morelos, and (3) Iguala, (4) Huitzuco, (5) Eduardo Neri (Xochipala), (6) Eduardo Neri (Zumpango), (7) Leonardo Bravo, and (8) Chilpancingo in Guerrero. *, capital city of the states and collecting areas in which hantavirus-negative (○) and -positive (●) rodents were detected.

Table 3
Total number and seropositive rodents captured in various localities in Morelos and Guerrero.

Rodent	Number captured	Ab positive (%)
Morelos		
Heteromys irroratus	2	0
Microtus mexicanus	15	0
Mus musculus	12	0
Neotoma alstoni	2	0
Neotoma mexicana	1	0
Peromyscus hylocetes	13	0
Peromyscus maniculatus	2	0
Reithrodontomys megalotis	25	2(8.0)
Guerrero		
Baiomys musculus	5	0
Heteromys irroratus	13	0
Heteromys pictus	5	0
Hodomys alleni	4	0
Megadontomys thomasi	9	1(11.1)
Neotoma picta	6	1(16.7)
Handleyomys alfaroi	3	0
Oryzomys couesi	16	0
Handleyomys melanotis	2	0
Osgoodomys banderanus	36	0
Peromyscus mexicanus	10	0
Peromyscus aztecus evides	1	1(100.0)
Peromyscus beatae	127	31(24.4)
Peromyscus lepturus	5	0
Peromyscus levipes	11	0
Peromyscus megalops	41	1(2.4)
Peromyscus melanocarpus	2	0
Peromyscus melanophrys	9	0
Peromyscus spp.	14	0
Ratus rattus	1	0
Reithrodontomys spp.	1	0
Reithrodontomys sumichrasti	15	6(40.0)
Sigmodon mascotensis	1	0
Tylomys nudicaudus	1	0
Total	410	43(10.5)

proportion of hantavirus-positive male and female rodents was 88.4% and 11.6%, respectively.

To assess the evolutionary relationship between the Mexican and other known hantaviruses, we constructed phylogenetic trees based on partial S segment sequences (Figs. 2 and S1) since efforts to obtain all full S segment sequences were not successful. The analysis revealed that all of the Mexican viruses identified in this study were monophyletic with other members in the Sigmodontinae/Neotominae subfamilies. The viruses were clustered into the three major clades (with high branch node support) of MTNV (95%), CARV (99%), and HUIV (98%). Compared to known sequences of MTNV, CARV, and HUIV, the first and largest monophyletic clade of 30 taxa determined in this study was composed exclusively of MTNV that were distinct from all other previously identified hantaviruses. The analysis placed six other sequences with CARV and a single sequence with HUIV. Analysis based on the full-length S segment ORFs gave similar results, supporting the observed tree topology (Fig. S1). A comparison of the virus S segment sequence identities showed that viruses within respective groups were closely related (Table 5). The nucleotide and deduced amino acid sequence similarity within the MTN viruses ranged from 96.6% to 100% and 99.0% to 100%, respectively, while that of Carrizal viruses was 98.4% to 100% and 99% to 100%, respectively. The single sequence (96/2006) derived from *P. beatae* was more closely related to HUIV and showed a nucleotide and amino acid similarity of 99.7% and 100%, respectively.

The phylogeny based on cyt*b* gene sequence analysis of hantavirus-positive rodents showed a topology that in general reflected that of the virus gene phylogeny (Fig. 3). The analysis showed that rodents hosting MTN viruses clustered together in a single, well-supported clade (node support, 100%), indicating that these viruses were all carried by *P. beatae* with one exception: MTNV (171/2007) was found in *P. aztecus evides*. Similarly,

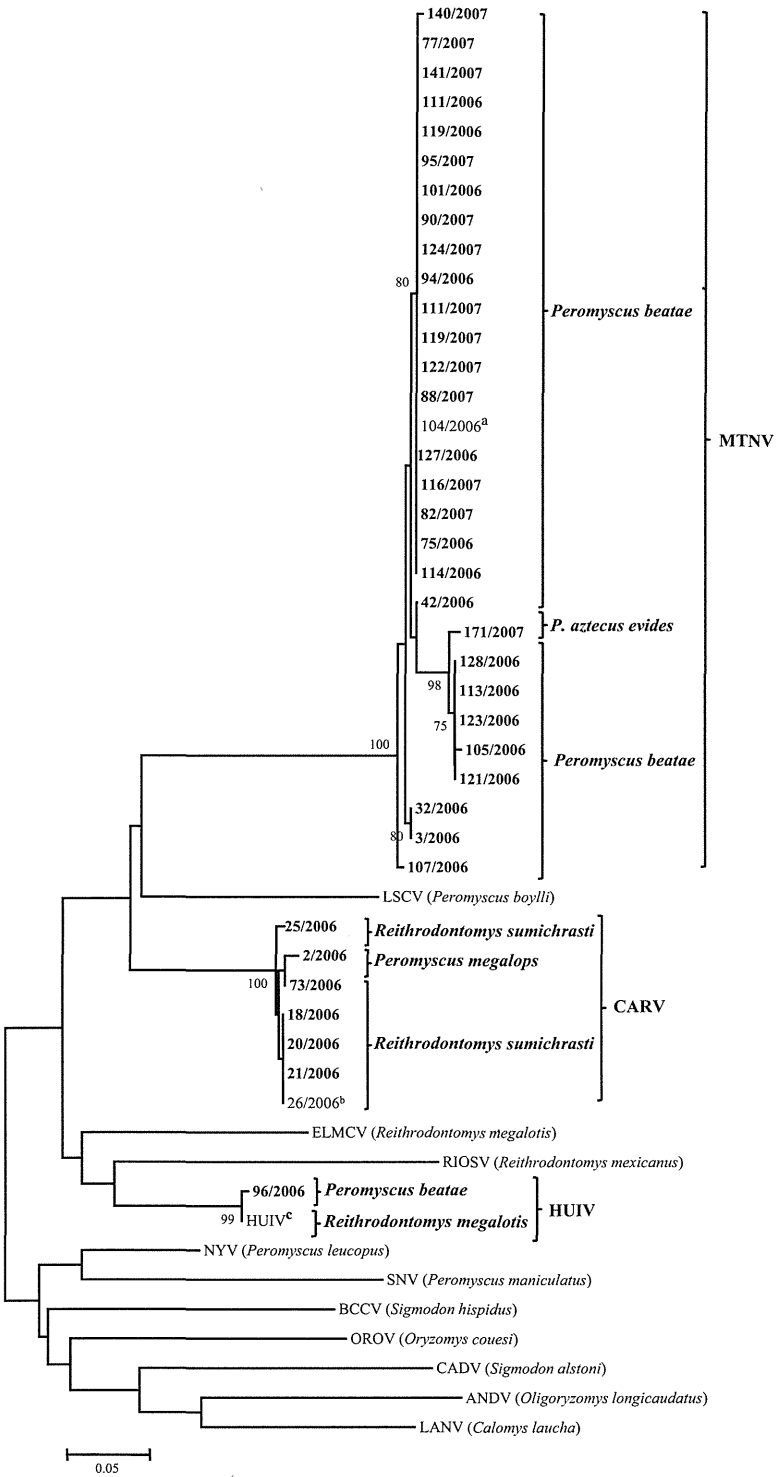

Fig. 2. A phylogenetic tree based on the partial S segment coding region was generated by the neighbor-joining (NJ) method using MEGA 4 software. The bootstrap consensus tree inferred from 1000 replicates was considered to represent the evolutionary history of the taxa ($n = 49$) analyzed. Branches corresponding to partitions reproduced in less than 70% of bootstrap replicates are not shown. In total, 312 positions were included in the final data set. The scale bar indicates the evolutionary distance of 0.05 substitutions per site. Sequences of Mexican hantavirus strains used in this study are shown in bold. Other GenBank database sequences used in the analysis are given in Table S2. a, b, and c were previously described as MTNV, CARV, and HUIV, respectively (Kariwa et al., 2012).

Table 4
Hantavirus infection in Mexican rodents.

Sample no.	Virus	Rodent	Collection site[a]	Sex	Ab	RNA	S segment	Cyt*b*
104/2006	**MTNV**	***P. beatae***	**7b**	**M**	–	**+**	**AB620100**	**AB618715**
3/2006	"	*P. beatae*	7a	M	+	+	AB620077	AB705157
32/2006	"	*P. beatae*	7a	M	+	+	AB620078	AB618643
42/2006	"	*P. beatae*	7a	M	+	+	AB620079	AB618723
75/2006	"	*P. beatae*	7c	M	+	+	AB620080	AB618710
77/2007	"	*P. beatae*	7e	M	+	+	AB703008	AB702996
82/2007	"	*P. beatae*	7e	M	+	+	AB703009	AB702997
88/2007	"	*P. beatae*	7e	M	+	+	AB703010	AB702998
90/2007	"	*P. beatae*	7e	M	+	+	AB703011	AB702999
94/2006	"	*P. beatae*	7b	M	+	+	AB620082	AB618712
95/2007	"	*P. beatae*	7d	M	+	+	AB703012	AB703000
101/2006	"	*P. beatae*	7b	M	+	+	AB620081	AB618714
105/2006	"	*P. beatae*	7b	F	+	+	AB620083	AB618644
107/2006	"	*P. beatae*	7b	M	+	+	AB620084	AB618716
111/2006	"	*P. beatae*	7b	M	+	+	AB620085	AB618717
111/2007	"	*P. beatae*	7d	M	+	+	AB703013	AB703002
113/2006	"	*P. beatae*	7b	M	+	+	AB620086	AB618718
114/2006	"	*P. beatae*	7b	M	+	+	AB620087	AB618719
116/2007	"	*P. beatae*	7d	M	+	+	AB703014	AB703003
119/2006	"	*P. beatae*[b]	7b	M	+	+	AB620088	AB705158
119/2007	"	*P. beatae*	7d	M	+	+	AB703015	ND
121/2006	"	*P. beatae*	7b	M	+	+	AB620089	AB618708
122/2007	"	*P. beatae*	7d	M	+	+	AB703016	AB703004
123/2006	"	*P. beatae*	7b	M	+	+	AB620090	AB618720
124/2007	"	*P. beatae*[b]	7d	M	+	+	AB703017	ND
127/2006	"	*P. beatae*	7b	F	+	+	AB620091	AB618721
128/2006	"	*P. beatae*	7b	F	+	+	AB620092	AB618722
140/2007	"	*P. beatae*	7d	M	+	+	AB703018	AB703005
141/2007	"	*P. beatae*	7d	M	+	+	AB703019	AB703006
171/2007	"	*P. aztecus evides*	8a	M	+	+	AB703020	AB703007
26/2006	**CARV**	***R. sumichrasti***	**7a**	**M**	**+**	**+**	**AB620103**	**AB618727**
2/2006	"	*P. megalops*	7a	M	–	+	AB620093	AB618709
18/2006	"	*R. sumichrasti*	7a	M	+	+	AB620094	AB618730
20/2006	"	*R. sumichrasti*	7a	M	+	+	AB620095	AB618731
21/2006	"	*R. sumichrasti*	7a	M	+	+	AB620096	AB618732
25/2006	"	*R. sumichrasti*	7a	F	+	+	AB620097	AB618726
73/2006	"	*R. sumichrasti*	7c	M	+	+	AB620098	AB618729
200/2006	**HUIV**	***R. megalotis***	**1a**	**M**	**+**	**+**	**AB620106**	**AB618725**
96/2006	"	*P. beatae*	7b	M	+	+	AB620099	AB618713
27/2006	ND	*N. picta*	**7a**	M	+	–	–	AB618728
92/2006	ND	*M. thomasi*	7c	M	+	–	–	AB618711
96/2007	ND	*P. beatae*	7d	M	+	–	–	AB703001
153/2006	ND	*R. megalotis*	1a	F	+	–	–	AB618724
Total		43			41	39		

ND, not determined.
[a] Numbers represent the collection site of rodents as described in Fig. 1 and Table 1.
[b] Rodent species identification only by morphology.

six of the seven CARV were detected in *R. sumichrasti*, except for CARV (2/2006), which was found in *P. megalops*. In addition, HUIV (96/2006) was detected in *P. beatae* but not in *R. megalotis* (Fig. 3).

To obtain more information on Mexican hantaviruses and their rodent hosts, we conducted epidemiological surveys in Morelos and Guerrero, Mexico. An earlier investigation identified three distinct hantaviruses circulating in Mexican wild rodents (Kariwa et al., 2012), which suggested the existence of several hantaviruses in the area. In this follow-up study, genetic analysis of virus and rodent host genes strongly indicated that *P. beatae* and *R. sumichrasti* are the primary reservoirs for MTNV and CARV, respectively.

During the two surveys, 410 rodents were trapped from eight different collecting areas, with the largest number (82%) captured in Guerrero. The high trapping rate (50%) in Carrizal de Bravo, with a high seroprevalence (20.0%), suggests a high rodent density with elevated levels of infection, a common occurrence in wild rodents (Calisher et al., 2007; Niklasson et al., 1995). *P. beatae* (127/339) and *R. megalotis* (25/72) were the predominant species at Guerrero and Morelos collecting points, respectively. The detection of antibodies and virus RNA indicate that the infected rodents species play a role as host species for hantaviruses (Childs et al., 1994). Our findings also suggest that *P. beatae* and *R. sumichrasti* are the primary hosts of MTNV and CARV, respectively. Detection of virus RNA in seropositive animals also indicates persistent infection and highlights the importance of these species in the maintenance and transmission of hantaviruses (Childs et al., 1994). Our recent rodent survey results conducted elsewhere highlighted the role of male rodents in the epidemiology of hantavirus (Daud et al., 2007).

Phylogenetic analysis of the virus and rodent gene sequences demonstrated the close association of MTNV with *P. beatae* and CARV with *R. sumichrasti*. As commonly observed with hantaviruses, this strong correlation suggests a coevolutionary relationship (Hughes and Friedman, 2000). With regard to HUIV, no firm conclusions were reached due to the constraints of a small sample size with regard to hantavirus-positive rodents. Some specific observations with sample 171/2007, a MTN virus detected in the Chilpancingo area in a *P. aztecus evides* rodent, may suggest spillover or otherwise the existence of different rodent species hosting the same virus (Morzunov et al., 1998; Nemirov et al., 2002). For example, two viruses, prototype MTNV (104/2006) identified

Table 5
Percentage nucleotide and amino acid similarity of partial S segment (321 bp) of Mexican hantaviruses and other known hantaviruses.

	MTNVs									CARVs			HUIVs		Others									
	*MTNV	75/2006	82/2007	114/2006	141/2007	42/2006	32/2006	123/2006	171/2007	*CARV	2/2006	25/2006	*HUIV	96/2006	ANDV	BCCV	CADV	ELMCV	LANV	LSCV	NYV	OROV	RIOSV	SNV
***MTNV**	-	100	100	100	100	99.4	99.1	97.2	96.9	82.9	82.2	82.6	80.1	79.8	76.0	76.6	75.7	79.1	75.7	80.7	80.1	76.9	77.9	75.0
75/2006	100	-	100	100	100	99.4	99.1	97.2	96.9	82.9	82.2	82.6	80.1	79.8	76.0	76.6	75.7	79.1	75.7	80.7	80.1	76.9	77.9	75.0
82/2007	100	100	-	100	100	99.4	99.1	97.2	96.9	82.9	82.2	82.6	80.1	79.8	76.0	76.6	75.7	79.1	75.7	80.7	80.1	76.9	77.9	75.0
114/2006	100	100	100	-	100	99.4	99.1	97.2	96.9	82.9	82.2	82.6	80.1	79.8	76.0	76.6	75.7	79.1	75.7	80.7	80.1	76.9	77.9	75.0
141/2007	100	100	100	100	-	99.4	99.1	97.2	96.9	82.9	82.2	82.6	80.1	79.8	76.0	76.6	75.7	79.1	75.7	80.7	80.1	76.9	77.9	75.0
42/2006	100	100	100	100	100	-	98.4	97.8	97.5	82.9	82.2	82.6	79.4	79.1	75.4	76.6	75.7	78.5	75.1	81.3	80.1	76.9	77.3	75.6
32/2006	99.0	99.0	99.0	99.0	99.0	99.0	-	96.9	96.6	83.2	82.9	82.9	80.7	80.4	76.9	76.9	76.3	79.4	75.4	81.0	80.7	77.6	78.5	74.4
123/2006	100	100	100	100	100	100	99.0	-	99.1	81.6	81.3	81.3	80.4	80.1	75.7	77.6	75.7	78.2	74.8	80.4	79.4	77.3	76.6	75.6
171/2007	100	100	100	100	100	100	99.0	100	-	81.9	81.6	81.6	80.1	79.8	75.4	77.6	76.3	78.5	75.1	81.0	79.8	77.3	76.6	76.6
***CARV**	92.2	92.2	92.2	92.2	92.2	92.2	93.2	92.2	92.2	-	99.1	98.8	86.6	86.3	76.0	76.9	77.3	83.2	78.5	84.1	80.7	78.8	81.9	79.1
2/2006	92.2	92.2	92.2	92.2	92.2	92.2	93.2	92.2	92.2	100	-	98.4	86.3	86.0	76.3	76.6	77.6	82.6	78.2	84.1	80.4	79.1	81.6	80.0
25/2006	91.2	91.2	91.2	91.2	91.2	91.2	92.2	91.2	91.2	99.0	99.0	-	85.7	85.4	75.4	76.3	76.3	82.2	78.2	83.8	80.1	78.5	81.3	78.5
***HUIV**	91.3	91.3	91.3	91.3	91.3	91.3	92.2	91.3	91.3	96.1	96.1	95.1	-	99.7	76.6	77.9	76.3	82.9	77.3	81.0	77.6	78.2	82.6	80.0
96/2006	91.3	91.3	91.3	91.3	91.3	91.3	92.2	91.3	91.3	96.1	96.1	95.1	100	-	76.3	78.2	76.0	83.2	76.9	80.7	77.9	78.5	82.9	79.7
ANDV	81.6	81.6	81.6	81.6	81.6	81.6	82.5	81.6	81.6	85.4	85.4	85.3	84.5	84.5	-	78.8	79.8	76.9	82.2	75.4	78.5	77.6	73.8	75.9
BCCV	85.4	85.4	85.4	85.4	85.4	85.4	86.4	85.4	85.4	85.4	85.4	85.3	88.4	88.4	90.3	-	78.2	81.3	80.1	76.3	81.3	79.1	77.3	79.4
CADV	78.6	78.6	78.6	78.6	78.6	78.6	79.6	78.6	78.6	83.5	83.5	84.2	82.5	82.5	89.3	84.5	-	79.8	80.4	76.9	80.7	80.7	75.7	79.7
ELMCV	90.3	90.3	90.3	90.3	90.3	90.3	91.3	90.3	90.3	94.2	94.2	93.1	97.1	97.1	85.4	89.3	82.5	-	77.6	79.1	79.1	81.0	80.7	77.5
LANV	79.6	79.6	79.6	79.6	79.6	79.6	80.6	79.6	79.6	84.5	84.5	84.3	84.5	84.5	92.2	88.4	90.3	83.5	-	78.2	77.9	78.2	76.3	78.8
LSCV	95.1	95.1	95.1	95.1	95.1	95.1	96.1	95.1	95.1	95.1	95.1	94.1	93.2	93.2	82.5	86.4	79.6	91.3	82.5	-	78.2	80.4	80.7	79.7
NYV	85.4	85.4	85.4	85.4	85.4	85.4	86.4	85.4	85.4	85.4	85.4	86.1	85.4	85.4	89.3	90.3	87.4	85.4	87.4	87.4	-	81.0	77.9	82.5
OROV	82.5	82.5	82.5	82.5	82.5	82.5	83.5	82.5	82.5	87.4	87.4	87.3	89.3	89.3	87.4	92.2	88.4	89.3	90.3	86.4	88.4	-	80.1	79.7
RIOSV	91.3	91.3	91.3	91.3	91.3	91.3	92.2	91.3	91.3	94.2	94.2	93.1	94.2	94.2	84.5	88.4	80.6	92.2	82.5	93.2	85.4	86.4	-	80.0
SNV	91.0	91.0	91.0	91.0	91.0	91.0	90.0	91.0	91.0	88.0	88.0	88.0	89.9	89.9	89.0	92.0	87.3	90.0	86.1	89.0	92.2	90.1	86.0	-

*Prototype Mexican hantaviruses MTNV (104/2006), CARV (26/2006) and HUIV (200/2006) (Kariwa et al., 2012).

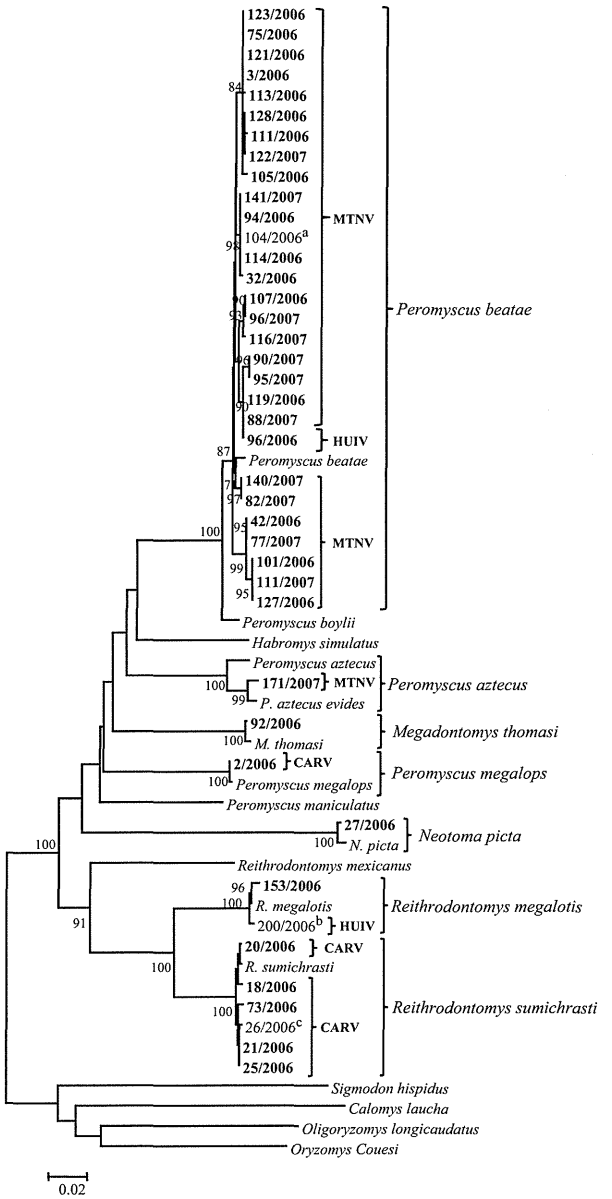

Fig. 3. A phylogenetic tree based on the partial mtDNA cyt*b* gene was generated by the neighbor-joining (NJ) method using MEGA 4 software. The bootstrap consensus tree inferred from 1000 replicates was considered to represent the evolutionary history of the taxa ($n = 57$) analyzed. Branches corresponding to partitions reproduced in less than 70% of bootstrap replicates are not shown. In total, 925 positions were included in the final data set. The scale bar indicates the evolutionary distance of 0.02 substitutions per site. Sequences of Mexican hantavirus strains used in this study are shown in bold: other GenBank database sequences used in the analysis are given in Table S2. a, b, and c were previously described as MTNV, HUIV, and CARV, respectively (Kariwa et al., 2012).

in *P. beatae* and MTNV (171/2007) detected in *P. aztecus evides*, were identified in two separate surveys, and their respective S segment ORFs had nucleotide and amino acid similarity of 96.9% and 100%, respectively, an indication that these were actually the same virus. Furthermore, the fact that these viruses were obtained from geographically distinct locations may indicate that the same virus was hosted by two different rodent species. Extensive sampling of rodents in this location would help clarify these observations.

The detection of CARV (2/2006) in *P. megalops* in the Carrizal area, where *R. sumichrasti* were the predominant rodents, suggest the possibility of spillover of this virus to *P. megalops*. In addition, lack of seroconversion suggested that this may have been a recent infection. Since HUIV (96/2006) was identified in *P. beatae*, in which MTNV was the predominant virus, it is tempting to speculate that a probable spillover event took place from *Reithrodontomys* species to *P. beatae*.

From these findings, the complex interactions of hantaviruses and their hosts have become evident. The role of these rodents in the epidemiology of Mexican hantaviruses may be extensive, and the virus–host relationship may be further complicated by obscure rodent taxonomy (Bradley et al., 2007). Previous seroprevalence studies have found other rodent species, such as *P. levipes*, *N. picta*, and *M. thomasi*, to be potential carriers of hantaviruses (Castro-Arellano et al., 2009; Mantooth et al., 2001). Additional work to detect viral RNA in these rodent species is needed, since attempts to amplify viral RNA in these rodents have been unsuccessful.

The importance of these Mexican hantaviruses as human pathogens still remains to be clarified. To date, unlike *Peromyscus*-borne viruses, *Reithrodontomys*-borne hantaviruses have not been linked to HPS in humans (Hjelle et al., 1994a, 1995). Screening for hantavirus-specific antibodies in local residents could provide data on the extent of exposure of humans to these potential pathogens.

Despite the relatively high number of infected rodents, the risk of these viruses to the local human population needs to be investigated, as no obvious correlation between rodent seroprevalence and human infection usually exists (Yates et al., 2002). Evidence obtained from this study highlights the importance of *P. beatae* and *R. sumichrasti* in the epidemiology of hantaviruses in Mexico. This study suggests the existence of an extensive relationship between Mexican rodents and hantaviruses, necessitating appropriate precautions that would minimize exposure to these rodents or their contaminated remains. Nevertheless, more studies are required to establish trends and dynamics in virus–rodent host interactions in the country. In addition, isolation of these Mexican viruses, although attempts have so far been unsuccessful, could provide opportunities for in-depth understanding of these hantaviruses.

This study provides valuable data toward understanding the epidemiology of Mexican hantaviruses and their hosts. Here, we report that *P. beatae* is the host for MTNV, and *R. sumichrasti* is the host for CARV.

Acknowledgments

We thank Dr. C.J. Peters for providing us with the construct for the expression of the nucleocapsid protein of SN virus. We also thank the students who worked with us in the field in Mexico for their assistance with rodent trapping. This work was financially supported by Grants-in-Aid for Scientific Research (16405034, 17255009, and 21405035) from the Ministry of Education, Culture, Sports, Science and Technology, Japan, and by a Health and Labor Sciences Research Grant on Emerging and Re-Emerging Infectious Diseases from the Japanese Ministry of Health, Labor and Welfare. This work was also supported by the Global COE Program for Zoonosis Control (Hokkaido University).

Appendix A. Supplementary data

Supplementary data associated with this article can be found, in the online version, at http://dx.doi.org/10.1016/j.virusres.2012.06.020.

References

Bradley, R.D., Durish, N.D., Rogers, D.S., Miller, J.R., Engstrom, M.D., Kilpatrick, C.W., 2007. Toward a molecular phylogeny for Peromyscus: evidence from mitochondrial cytochrome-b sequences. Journal of Mammalogy 88 (5), 1146–1159.

Calisher, C.H., Wagoner, K.D., Amman, B.R., Root, J.J., Douglass, R.J., Kuenzi, A.J., Abbott, K.D., Parmenter, C., Yates, T.L., Ksiazek, T.G., Beaty, B.J., Mills, J.N., 2007. Demographic factors associated with prevalence of antibody to Sin Nombre virus in deer mice in the western United States. Journal of Wildlife Diseases 43 (1), 1–11.

Castro-Arellano, I., Suzan, G., Leon, R.F., Jimenez, R.M., Lacher Jr., T.E., 2009. Survey for antibody to hantaviruses in Tamaulipas, Mexico. Journal of Wildlife Diseases 45 (1), 207–212.

Childs, J.E., Ksiazek, T.G., Spiropoulou, C.F., Krebs, J.W., Morzunov, S., Maupin, G.O., Gage, K.L., Rollin, P.E., Sarisky, J., Enscore, R.E., et al., 1994. Serologic and genetic identification of *Peromyscus maniculatus* as the primary rodent reservoir for a new hantavirus in the southwestern United States. Journal of Infectious Diseases 169 (6), 1271–1280.

Chu, Y.-K., Owen, R.D., Sanchez-Hernandez, C., Romero-Almaraz, M.d.L., Jonsson, C.B., 2008. Genetic characterization and phylogeny of a hantavirus from Western Mexico. Virus Research 131 (2), 180–188.

Daud, N.H., Kariwa, H., Tanikawa, Y., Nakamura, I., Seto, T., Miyashita, D., Yoshii, K., Nakauchi, M., Yoshimatsu, K., Arikawa, J., Takashima, I., 2007. Mode of infection of Hokkaido virus (Genus Hantavirus) among grey red-backed voles, *Myodes rufocanus*, in Hokkaido, Japan. Microbiology and Immunology 51 (11), 1081–1090.

Felsenstein, J., 1985. Confidence limits on phylogenies: an approach using the bootstrap. Evolution 39, 783–791.

Hjelle, B., Anderson, B., Torrez-Martinez, N., Song, W., Gannon, W.L., Yates, T.L., 1995. Prevalence and geographic genetic variation of hantaviruses of new world harvest mice (Reithrodontomys): identification of a divergent genotype from a Costa Rican *Reithrodontomys mexicanus*. Virology 207 (2), 452–459.

Hjelle, B., Chavez-Giles, F., Torrez-Martinez, N., Yates, T., Sarisky, J., Webb, J., Ascher, M., 1994a. Genetic identification of a novel hantavirus of the harvest mouse *Reithrodontomys megalotis*. Journal of Virology 68 (10), 6751–6754.

Hjelle, B., Jenison, S., Torrez-Martinez, N., Yamada, T., Nolte, K., Zumwalt, R., MacInnes, K., Myers, G., 1994b. A novel hantavirus associated with an outbreak of fatal respiratory disease in the southwestern United States: evolutionary relationships to known hantaviruses. Journal of Virology 68 (2), 592–596.

Hughes, A.L., Friedman, R., 2000. Evolutionary diversification of protein-coding genes of hantaviruses. Molecular Biology and Evolution 17 (10), 1558–1568.

Johnson, A.M., Bowen, M.D., Ksiazek, T.G., Williams, R.J., Bryan, R.T., Mills, J.N., Peters, C.J., Nichol, S.T., 1997. Laguna Negra virus associated with HPS in western Paraguay and Bolivia. Virology 238 (1), 115–127.

Jonsson, C.B., Figueiredo, L.T., Vapalahti, O., 2010. A global perspective on hantavirus ecology, epidemiology, and disease. Clinical Microbiology Reviews 23 (2), 412–441.

Kang, H.J., Bennett, S.N., Dizney, L., Sumibcay, L., Arai, S., Ruedas, L.A., Song, J.W., Yanagihara, R., 2009. Host switch during evolution of a genetically distinct hantavirus in the American shrew mole (*Neurotrichus gibbsii*). Virology 388 (1), 8–14.

Kariwa, H., Yoshida, H., Sánchez-Hernández, C., Romero-Almaraz Mde, L., Almazán-Catalán, J.A., Ramos, C., Miyashita, D., Seto, T., Takano, A., Totani, M., Murata, R., Saasa, N., Ishizuka, M., Sanada, T., Yoshii, K., Yoshimatsu, K., Arikawa, J., Takashima, I., 2012. Genetic diversity of hantaviruses in Mexico: identification of three novel hantaviruses from Neotominae rodents. Virus Research 163 (2), 486–494.

Lee, H.W., Baek, L.J., Johnson, K.M., 1982. Isolation of Hantaan virus, the etiologic agent of Korean hemorrhagic fever, from wild urban rats. Journal of Infectious Diseases 146 (5), 638–644.

Levis, S., Morzunov, S.P., Rowe, J.E., Enria, D., Pini, N., Calderon, G., Sabattini, M., St. Jeor, S.C., 1998. Genetic diversity and epidemiology of hantaviruses in Argentina. Journal of Infectious Diseases 177 (3), 529–538.

Mantooth, S.J., Milazzo, M.L., Bradley, R.D., Hice, C.L., Ceballos, G., Tesh, R.B., Fulhorst, C.F., 2001. Geographical distribution of rodent-associated hantaviruses in Texas. Journal of Vector Ecology 26 (1), 7–14.

Martinez, V.P., Bellomo, C., San Juan, J., Pinna, D., Forlenza, R., Elder, M., Padula, P.J., 2005. Person-to-person transmission of Andes virus. Emerging Infectious Diseases 11 (12), 1848–1853.

Milazzo, M.L., Cajimat, M.N., Hanson, J.D., Bradley, R.D., Quintana, M., Sherman, C., Velasquez, R.T., Fulhorst, C.F., 2006. Catacamas virus, a hantaviral species naturally associated with *Oryzomys couesi* (Coues' oryzomys) in Honduras. American Journal of Tropical Medicine and Hygiene 75 (5), 1003–1010.

Morzunov, S.P., Feldmann, H., Spiropoulou, C.F., Semenova, V.A., Rollin, P.E., Ksiazek, T.G., Peters, C.J., Nichol, S.T., 1995. A newly recognized virus associated with a fatal case of hantavirus pulmonary syndrome in Louisiana. Journal of Virology 69 (3), 1980–1983.

Morzunov, S.P., Rowe, J.E., Ksiazek, T.G., Peters, C.J., St Jeor, S.C., Nichol, S.T., 1998. Genetic analysis of the diversity and origin of hantaviruses in *Peromyscus leucopus* mice in North America. Journal of Virology 72 (1), 57–64.

Nemirov, K., Henttonen, H., Vaheri, A., Plyusnin, A., 2002. Phylogenetic evidence for host switching in the evolution of hantaviruses carried by Apodemus mice. Virus Research 90 (1–2), 207–215.

Niklasson, B., Hornfeldt, B., Lundkvist, A., Bjorsten, S., Leduc, J., 1995. Temporal dynamics of Puumala virus antibody prevalence in voles and of nephropathia epidemica incidence in humans. American Journal of Tropical Medicine and Hygiene 53 (2), 134–140.

Okumura, M., Yoshimatsu, K., Kumperasart, S., Nakamura, I., Ogino, M., Taruishi, M., Sungdee, A., Pattamadilok, S., Ibrahim, I.N., Erlina, S., Agui, T., Yanagihara, R., Arikawa, J., 2007. Development of serological assays for Thottapalayam virus, an insectivore-borne Hantavirus. Clinical and Vaccine Immunology 14 (2), 173–181.

Padula, P., Figueroa, R., Navarrete, M., Pizarro, E., Cadiz, R., Bellomo, C., Jofre, C., Zaror, L., Rodriguez, E., Murua, R., 2004. Transmission study of Andes hantavirus infection in wild sigmodontine rodents. Journal of Virology 78 (21), 11972–11979.

Padula, P.J., Edelstein, A., Miguel, S.D., Lopez, N.M., Rossi, C.M., Rabinovich, R.D., 1998. Hantavirus pulmonary syndrome outbreak in Argentina: molecular evidence for person-to-person transmission of Andes virus. Virology 241 (2), 323–330.

Rollin, P.E., Ksiazek, T.G., Elliott, L.H., Ravkov, E.V., Martin, M.L., Morzunov, S., Livingstone, W., Monroe, M., Glass, G., Ruo, S., et al., 1995. Isolation of black creek canal virus, a new hantavirus from *Sigmodon hispidus* in Florida. Journal of Medical Virology 46 (1), 35–39.

Rowe, J.E., St. Jeor, S.C., Riolo, J., Otteson, E.W., Monroe, M.C., Henderson, W.W., Ksiazek, T.G., Rollin, P.E., Nichol, S.T., 1995. Coexistence of several novel hantaviruses in rodents indigenous to North America. Virology 213 (1), 122–130.

Saitou, N., Nei, M., 1987. The neighbor-joining method: a new method for reconstructing phylogenetic trees. Molecular Biology and Evolution 4 (4), 406–425.

Schmaljohn, C.S., Schmaljohn, A.L., Dalrymple, J.M., 1987. Hantaan virus M RNA: coding strategy, nucleotide sequence, and gene order. Virology 157 (1), 31–39.

Song, J.W., Baek, L.J., Gajdusek, D.C., Yanagihara, R., Gavrilovskaya, I., Luft, B.J., Mackow, E.R., Hjelle, B., 1994. Isolation of pathogenic hantavirus from white-footed mouse (*Peromyscus leucopus*). Lancet 344 (8937), 1637.

Suzan, G., Ceballos, G., Mills, J., Ksiazek, T.G., Yates, T., 2001. Serologic evidence of hantavirus infection in sigmodontine rodents in Mexico. Journal of Wildlife Diseases 37 (2), 391–393.

Tamura, K., Dudley, J., Nei, M., Kumar, S., 2007. MEGA4: Molecular Evolutionary Genetics Analysis (MEGA) software version 4.0. Molecular Biology and Evolution 24 (8), 1596–1599.

Tamura, K., Nei, M., Kumar, S., 2004. Prospects for inferring very large phylogenies by using the neighbor-joining method. Proceedings of the National Academy of Sciences of the United States of America 101 (30), 11030–11035.

Yates, T., Mills, J., Parmenter, C., Ksiazek, T., Parmenter, R., Vande Castle, J., Calisher, C., Nichol, S., Abbot, K., Young, J., Morrison, M., Beaty, B., Dunnum, J., Baker, R., Salazar-Bravo, J., Peters, C., 2002. The ecology and evolutionary history of an emergent disease: hantavirus pulmonary syndrome. BioScience 52 (11), 989–998.

Zeitz, P.S., Butler, J.C., Cheek, J.E., Samuel, M.C., Childs, J.E., Shands, L.A., Turner, R.E., Voorhees, R.E., Sarisky, J., Rollin, P.E., et al., 1995. A case–control study of hantavirus pulmonary syndrome during an outbreak in the southwestern United States. Journal of Infectious Diseases 171 (4), 864–870.

Virology 428 (2012) 48–57

Contents lists available at SciVerse ScienceDirect

Virology

journal homepage: www.elsevier.com/locate/yviro

The N-terminus of the Montano virus nucleocapsid protein possesses broadly cross-reactive conformation-dependent epitopes conserved in rodent-borne hantaviruses

Ngonda Saasa [a,e], Haruka Yoshida [a], Kenta Shimizu [d], Cornelio Sánchez-Hernández [b], María de Lourdes Romero-Almaraz [b], Takaaki Koma [d], Takahiro Sanada [a], Takahiro Seto [a], Kentaro Yoshii [a], Celso Ramos [c], Kumiko Yoshimatsu [d], Jiro Arikawa [d], Ikuo Takashima [a], Hiroaki Kariwa [a,*]

[a] Laboratory of Public Health, Graduate School of Veterinary Medicine, Hokkaido University, Kita-18, Nishi-9, Kita-Ku, Sapporo 060-0818, Hokkaido, Japan
[b] Instituto de Biologia, Universidad Nacional Autónoma de México, Mexico
[c] Instituto Nacional de Salud Pública, Cuernavaca, Morelos, Mexico
[d] Department of Microbiology, Hokkaido University Graduate School of Medicine, Japan
[e] Department of Disease Control, University of Zambia School of Veterinary Medicine, Zambia

ARTICLE INFO

Article history:
Received 21 December 2011
Returned to author for revisions
19 January 2012
Accepted 13 March 2012
Available online 19 April 2012

Keywords:
Hantavirus
Montano virus
Nucleocapsid protein
Monoclonal antibody
Conformational epitope
Cross-reactivity

ABSTRACT

The hantavirus nucleocapsid (N) protein is an important immunogen that stimulates a strong and cross-reactive immune response in humans and rodents. A large proportion of the response to N protein has been found to target its N-terminus. However, the exact nature of this bias towards the N-terminus is not yet fully understood. We characterized six monoclonal antibodies (mAbs) against the N protein of Montano virus (MTNV), a Mexican hantavirus. Five of these mAbs recognized eight American hantaviruses and six European and Asian hantaviruses, but not the Soricomorpha-borne Thottapalayam hantavirus. The N protein-reactive binding regions of the five mAbs were mapped to discontinuous epitopes within the N-terminal 13–51 amino acid residues, while a single serotype-specific mAb was mapped to residues 1–25 and 49–75. Our findings suggest that discontinuous epitopes at the N-terminus are conserved, at least in rodent-borne hantaviruses, and that they contribute considerably to N protein cross-reactivity.

Introduction

The hantavirus (family *Bunyaviridae*) genome consists of three RNA segments of negative-sense polarity, Large (L), Medium (M), and Small (S), encoding the viral polymerase, envelope glycoproteins, and nucleocapsid (N) protein, respectively (Schmaljohn et al., 1986). Hantaviruses are normally carried by persistently infected rodents, from which humans are believed to acquire the infection primarily through the inhalation of virus-contaminated excreta; however, human-to-human transmission has also been reported (Martinez et al., 2005). Infection with American hantaviruses causes hantavirus pulmonary syndrome (Hjelle et al., 1994), whereas the viruses originating from Europe and Asia cause hemorrhagic fever with renal syndrome (Avsic-Zupanc et al., 1992).

European and Asian (i.e., Old World) hantaviruses known to cause illness in humans include Hantaan virus (HTNV), Dobrava virus (DOBV), Puumala virus (PUUV), Seoul virus (SEOV), and Amur virus (AMRV). Others, such as Tula virus (TULV) and Hokkaido virus (HOKV), have not been associated with human disease. American (i.e., New World) hantaviruses, such as Sin Nombre virus (SNV), New York virus (NYV), Black Creek Canal virus (BCCV), and Bayou virus (BAYV), are known human pathogens. In South America, viruses so far linked with human illness include Andes virus (ANDV), Laguna Negra virus (LANV), and Lechiguanas virus (LECV). Maporal virus (MAPV), Rio Mamore virus (RIOMV), have not been associated with human disease (Jonsson et al., 2010).

Hantaviruses detected in Mexico include EL Moro Canyon virus (ELMCV) (Torrez-Martinez et al., 1995) and, more recently, Playa de Oro virus (OROV) (Chu et al., 2008). In our recent wild rodent epidemiological survey in Guererro and Morelos States, Mexico, we identified virus RNA of three distinct hantaviruses, currently designated as Montano virus (MTNV), Carrizal virus (CARV), and Huitzilac virus (HUIV), the pathogenicity of which to humans is still unknown (Kariwa et al., 2012).

The hantavirus N protein, in addition to being the most abundant viral protein, plays key roles in hantavirus infection, including encapsidation, binding of the viral RNA genome (Severson et al., 2001; Xu et al., 2002), and initiation of the transcription and

* Corresponding author. Fax: +81 11 706 5213.
E-mail address: kariwa@vetmed.hokudai.ac.jp (H. Kariwa).

0042-6822/$ - see front matter © 2012 Elsevier Inc. All rights reserved.
http://dx.doi.org/10.1016/j.virol.2012.03.001

translation of viral mRNA (Cheng et al., 2011; Severson et al., 2005). The N-terminus of the N protein has been found to be necessary for other viral processes, including oligomerization and N–N interactions (Alminaite et al., 2006; Kaukinen et al., 2001). The N protein is a frequently used antigen for detecting hantavirus antibodies, because it is highly conserved and provokes a strong immune response in humans and mice (Bharadwaj et al., 2000; de Carvalho Nicacio et al., 2002). Although antigenic determinants have been detected over the entire length of the N protein, the strongest response is directed toward the N-terminus (Alfadhli et al., 2002; Boudko et al., 2007; Elgh et al., 1996; Jenison et al., 1994; Lundkvist et al., 1996), which contributes substantially to the overall cross-reactive immune response (Lindkvist et al., 2007; Tischler et al., 2008). As such, deletion of the N-terminus from the protein permits the generation of antigens with serotype-specific applications (Koma et al., 2010; Li et al., 2006; Morii et al., 1998; Tischler et al., 2008).

Monoclonal antibodies (mAbs) are useful tools for studying hantavirus antigenic characteristics due to their specificity. So far, several studies have attempted to generate mAbs with desired specificities. For example, the immunization of mice with more than one antigen or the use of virus core particle delivery systems have generated mAbs with relatively broad cross-reactivity (Geldmacher et al., 2004; Kucinskaite-Kodze et al., 2011). A large proportion of this response was shown to arise from the N-terminus. Evidence gathered through crystal structural analysis and nuclear magnetic resonance (NMR) spectroscopic predictions have revealed that the N-terminus assumes a coiled-coil α-helix conformation (Boudko et al., 2007; Wang et al., 2008). However, the role of this domain in inducing strong and cross-reactive responses remains to be thoroughly investigated.

To broaden our understanding of the antigenic properties of the N protein of Mexican hantavirus, we generated and characterized six mAbs against MTNV N protein expressed in bacteria. Five of the six mAbs showed a strong and broad spectrum of reactivity to both American and Eurasian rodent-borne hantaviruses (reactivity to the Soricomorpha-borne Thottapalayam virus [TPMV] was not observed). The binding regions of the five cross-reactive mAbs were mapped to the N-terminal 13–51 amino acids (aas) of the N protein, with their activity apparently dependent on the preservation of the integrity of the N-terminal domain. Our findings suggest that the N protein coiled-coil α-helix domain possesses conformational epitopes that contribute significantly to cross-reactivity, at least in rodent-borne hantaviruses.

Results

mAb production and isotyping

Six hybridoma clones (2H10, 9E5, 10G5, 2F11, 7E6, and G8B4) that had a strong and specific reaction to MTNV N protein on enzyme-linked immunosorbent assay (ELISA) were established. All six mAbs recognized the hantavirus N protein by Western blotting. All clones were of the IgG1 Kappa subclass except for 10G5, which belonged to IgG2a (Supplementary Table 1).

Reactivity of the mAbs to bacteria- and baculovirus-expressed hantavirus N protein

To determine the extent of mAb reactivity to different hantaviruses, several N proteins expressed in bacteria or a baculovirus system were tested by ELISA. The mAbs recognized bacterially-expressed whole N proteins of homologous MTNV and two other Mexican hantaviruses (HUIV and CARV), as well as SNV (Fig. 1A). The reactivity of the mAbs to the European and Asian hantavirus N antigens was varied. For example, mAb 2H10, 10G5 and 7E6 recognized and reacted with nearly all of the antigens, including ANDV, LANV, MAPV, HTNV, SEOV, AMRV, PUUV, TULV, and HOKV [AB010731]. All of the mAbs except G8B4 also reacted with the N proteins of PUUV, TULV and HOKV whereas 2F11 did not recognize the HTNV, AMRV and SEOV antigens and 9E5 did not react with AMRV and SEOV. G8B4 showed specificity to North American hantaviruses, reacting only with SNV and the three

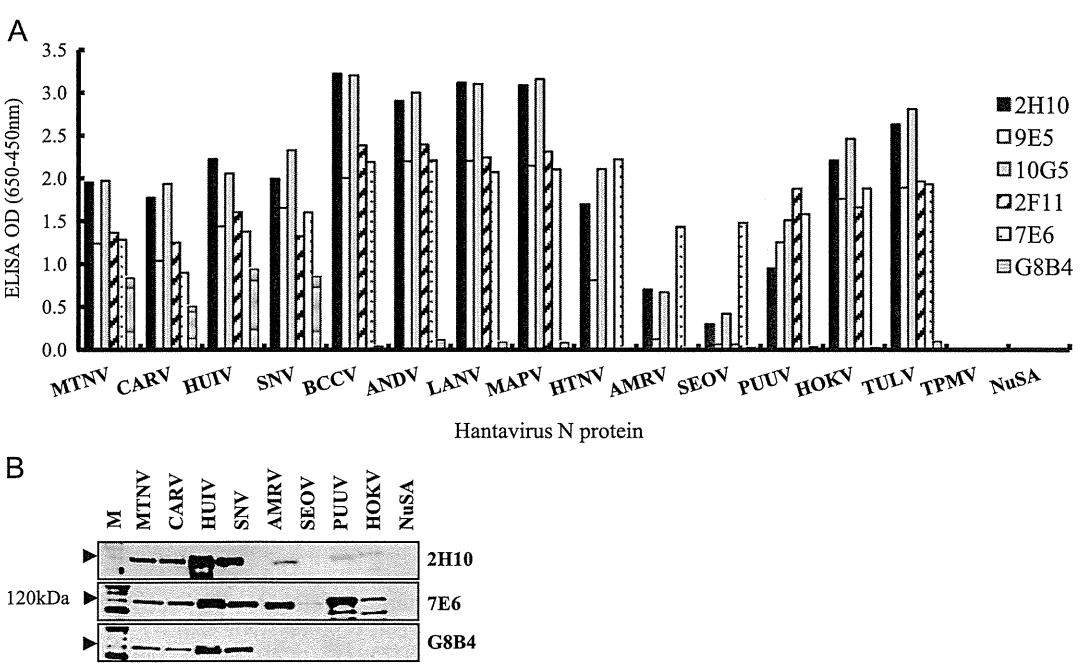

Fig. 1. Reactivity of mAbs to whole hantavirus N protein fused with NuSA (~120 kDa). (A) ELISA reactivity of mAbs to 15 hantavirus N proteins and NuSA as a negative control antigen and (B) reactivity of 2H10, 7E6 and G8B4 to the hantavirus N proteins on Western blotting.

Table 1
Reactivities of mAbs to N proteins of hantaviruses expressed in baculovirus in ELISA.

mAb	North America					South America			Europe and Asia				
	MTNV	CARV	HUIV	SNV	BCCV	ANDV	LANV	MAPV	HTNV	SEOV	PUUV	TULV	TPMV
2H10	+[a]	+	+	+	+	+	+	+	+	+	+	+	−[b]
9E5	+	+	+	+	+	+	+	+	+	+	+	+	−
10G5	+	+	+	+	+	+	+	+	+	+	+	+	−
2F11	+	+	+	+	+	+	+	+	−	−	+	+	−
7E6	+	+	+	+	+	+	+	+	+	+	+	+	−
G8B4	+	−	−	−	−	−	−	−	−	−	−	−	−

[a] ELISA OD: ≥0.2.
[b] ELISA OD: <0.2.

Table 2
Reactivities of mAbs to N proteins of hantaviruses expressed in Vero E6 cells on IFA.

Region	North America				South America			Europe and Asia				
N protein	MTNV	CARV	HUIV	SNV	ANDV	LANV	MAPV	HTNV	SEOV	PUUV	TULV	TPMV
2H10	+[a]	+	+	+	+	+	+	+	+	+	+	−[b]
9E5	+	+	+	+	+	+	+	+	+	+	+	−
10G5	+	+	+	+	+	+	+	+	+	+	+	−
2F11	+	+	+	+	+	+	+	−	−	+	+	−
7E6	+	+	+	+	+	+	+	+	+	+	+	−
G8B4	+	+	+	+	−	+	+	−	−	−	+	−
E5G6[c]	+	−	+	+	+	+	+	+	+	+	+	+[d]

[a] IFA titer: ≥1:100.
[b] IFA titer: <1:100.
[c] Hybridoma culture supernatant.
[d] TMPV N was manipulated to add binding ability to E5G6 (Okumura et al., 2007).

Mexican hantaviruses (MTNV, CARV, and HUIV) although not with BCCV antigen. The reactivity of representative mAbs to bacterially-expressed hantavirus N proteins was confirmed by a strong response on Western blotting. None of the mAbs reacted with NuSA, a negative control antigen (Fig. 1B).

We also examined the reactivity to baculovirus-derived N proteins of various hantaviruses (Table 1). Four of the mAbs (2H10, 9E5, 10G5, and 7E6) recognized baculovirus-derived antigens of North (MTNV, CARV, HUIV, SNV, and BCCV) and South American hantaviruses (ANDV, LANV, and MAPV) as well as the European and Asian viruses (HTNV, SEOV, PUUV, and TULV) but not TPMV. The mAb 2F11 did not react with HTNV or SEOV antigen. G8B4 reacted with homologous MTNV N antigen but did not react with other N proteins examined, including the closely related CARV, HUIV or SNV antigen.

Reactivity of the mAbs to native hantavirus N proteins expressed in Vero E6 cells by indirect immunofluorescence antibody assay (IFA)

The reactivity of the mAbs to native antigens was further assessed by IFA in transfected and infected Vero E6 cells. The mAb reactivity pattern was consistent between the N proteins in both transfected and infected cells. As summarized in Table 2, the five cross-reactive mAbs strongly recognized nearly all American, European, and Asian hantavirus N proteins tested. However, 2F11 did not react with the HTNV or SEOV antigens, while G8B4 only reacted with the N proteins of MTNV, CARV, HUIV, SNV, and weakly to LANV, MAPV and TULV. A manipulated TPMV N protein to add the binding ability to E5G6 was used to confirm expression (Okumura et al., 2007).

The reactivity on IFA was verified by applying the mAbs to authentic hantavirus N protein in virus-infected cells, in which a response similar to that in transfected cells was observed (Table 3). None of the mAbs reacted with TPMV N protein (Tables 2 and 3).

Table 3
Reactivities of mAbs to authentic N proteins of European and Asian hantaviruses in IFA.

mAb	Rodent-borne				Soricomorpha-borne
	HTNV	SEOV	PUUV	TULV	TPMV
2H10	+[a]	+	+	+	−[b]
9E5	+	+	+	+	−
10G5	+	+	+	+	−
2F11	−	+	+	+	−
7E6	+	+	+	+	−
G8B4	−	−	−	+	−
E5G6[c]	+	+	+	+	+[d]

[a] IFA titer: ≥1:100.
[b] IFA titer: <1:100.
[c] Hybridoma culture supernatant.
[d] Anti-TPMV serum.

Determination of the binding regions using truncated MTNV N protein

Given the observed propensity of the mAbs for cross-reactivity to different hantavirus N proteins, we sought to define the regions of the N protein targeted by each mAb. Initially, we applied the mAbs to truncated MTNV N proteins (Fig. 2A). The mAbs recognized the whole N protein (N1–428), N1–80, and N1–150, but not N46–125, N125–275, or N250–428 (Table 4), suggesting that all of the epitopes were located within the first 80 aa residues at the N-terminus.

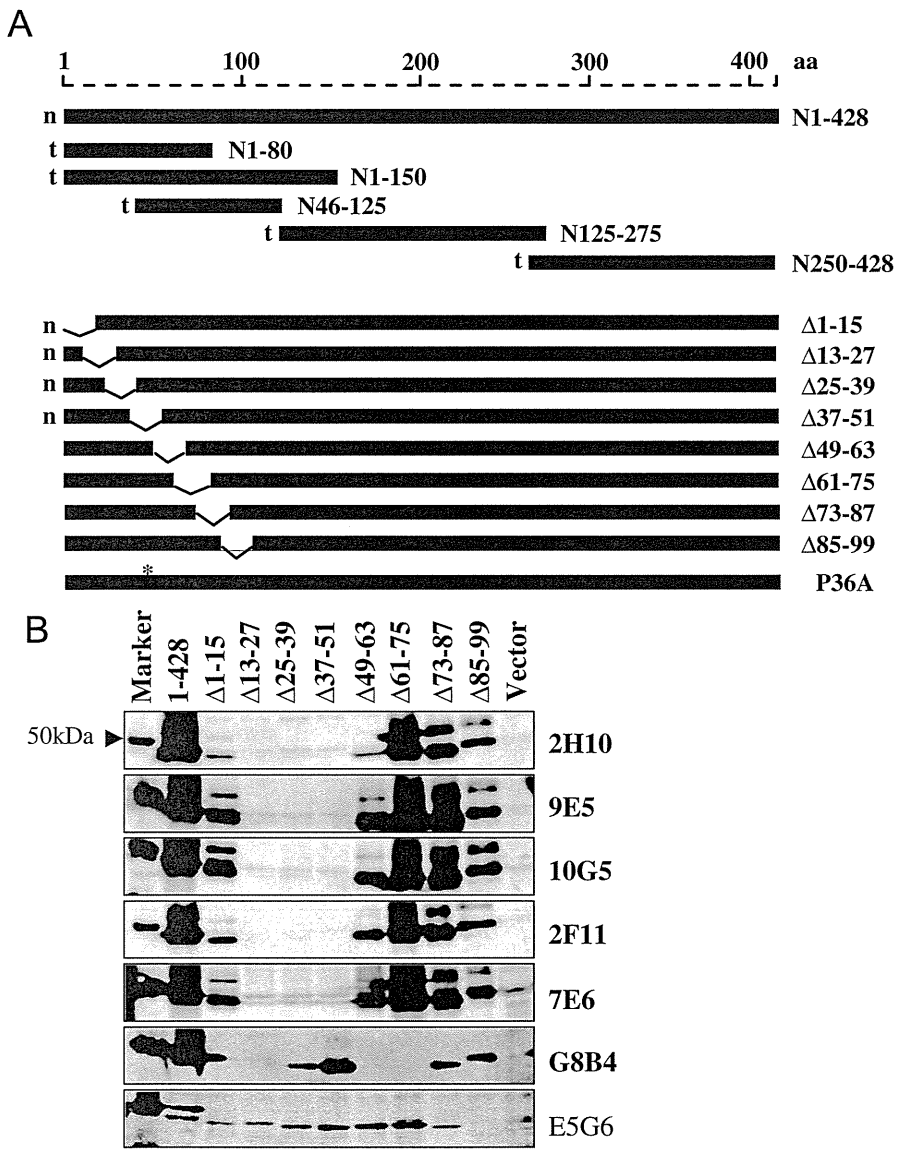

Fig. 2. Diagrammatic representation of MTNV N protein for mapping the epitopes recognized by the mAbs. (A) Full-length N protein and the truncated mutants, N protein mutants with 15aa deletions within the first 100 aas at the N-terminus. Substitution of alanine for proline at residue 36 (P36A) in full-length MTNV N protein. The n and t represent the N fusion protein for antigens expressed in bacteria. The asterisk (*) indicates the position of the alanine substitution in the N-terminus. (B) Assessment of the expression levels of the various N terminus deletion mutant constructs to the six mAbs compared to control mAb E5G6 with a binding region located outside the N-terminus.

Table 4
Reactivities of mAbs to bacterially-expressed full-length and truncated N proteins of MTNV.

mAb	MTNV N protein					
	N1–428	N1–80	N1–150	N46–125	N125–275	N250–428
2H10	+[a]	+	+	−[b]	−	−
9E5	+	+	+	−	−	−
10G5	+	+	+	−	−	−
2F11	+	+	+	−	−	−
7E5	+	+	+	−	−	−
G8B4	+	+	+	−	−	−

[a] ELISA OD: ≥ 0.2.
[b] ELISA OD: < 0.2.

Determination of the binding regions using MTNV N protein deletion fragments

To refine the binding regions of the mAbs within the N-terminus, we constructed and expressed 15 aa-deleted fragments of MTNV N protein covering residues 1–99 with three overlapping residues (Fig. 2A) and analyzed their reactivity by IFA (Table 5). Two major mAb patterns of reactivity were observed. Five mAbs (2H10, 9E5, 10G5, 2F11, and 7E6) recognized Δ1–15-deleted N but lost reactivity to Δ25–39 and Δ37–51 N, although 2F11 and 10G5 reacted weakly with Δ13–27 N. On the other hand, G8B4 showed a different response pattern: recognition was abolished by the Δ1–15 and Δ13–27 deletions, but restored by Δ25–39 and Δ37–51 N successive deletions, while Δ49–63 and Δ61–75 N

Table 5
Mapping of mAbs-binding regions to N protein of MTNV mutant N lacking 15 amino acids were expressed in Vero E6 cells and used as antigen for IFA test.

mAb	MTNV N Protein									Binding site (aa)
	N1–428	Δ1–15	Δ13–27	Δ25–39	Δ37–51	Δ49–63	Δ61–75	Δ73–87	Δ85–99	
2H10	+[a]	+	−[b]	−	−	+	+	+	+	13–51
9E5	+	+	−	−	−	+	+	+	+	13–51
10G5	+	+	+	−	−	+	+	+	+	25–51
2F11	+	+	+	−	−	+	+	+	+	25–51
7E6	+	+	−	−	−	+	+	+	+	13–51
G8B4	+	−	−	+	+	−	−	+	+	1–27, 49–75
E5G6[c]	+	+	+	+	+	+	+	+	+	166–175

[a] IFA titer: ≥1:100.
[b] IFA titer: <1:100.
[c] Hybridoma culture supernatant.

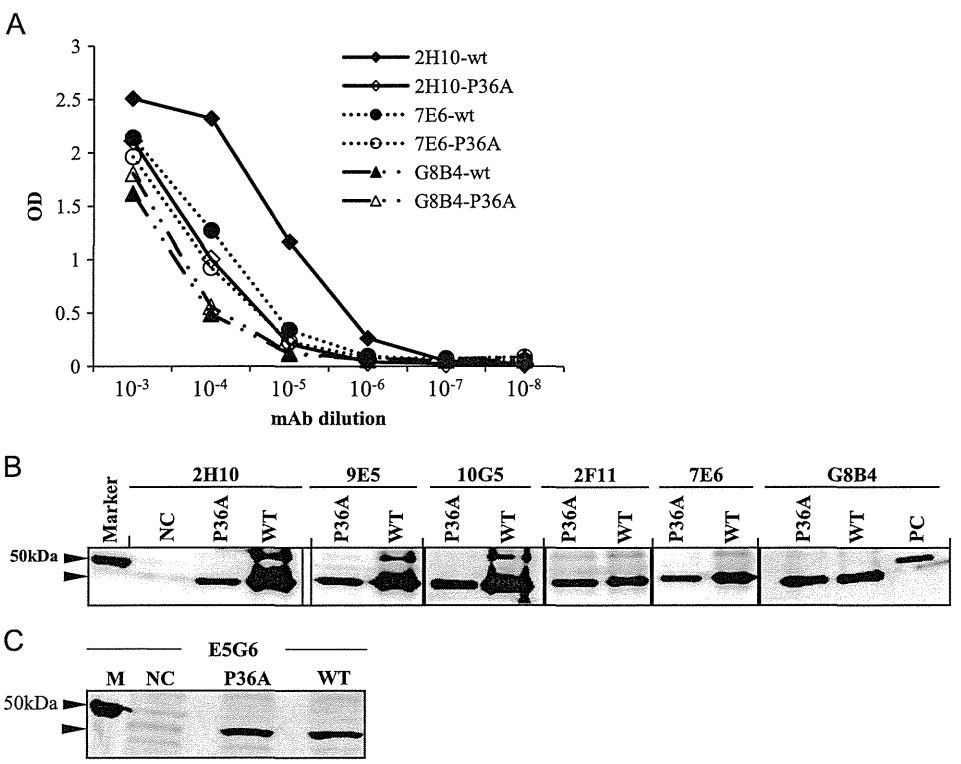

Fig. 3. Evaluation of mAb reactivity to wild-type MTNV N protein (wt) and P36A N protein as a 293T cell antigen lysate. (A) Indirect capture ELISA of biotinylated 2H10 (0.690 mg/mL), 7E6 (0.166 mg/mL), and G8B4 (0.138 mg/mL). (B) Assessment of the reactivity of the six mAbs to P36A N protein mutant and wild-type MTNV N protein (wt) and SNV N protein as a positive control (PC) on Western blotting. (C) Assessing the expression levels of the mutant N protein compared to the wt form using mAb E5G6 with a binding region located outside the N-terminus, empty vector as a negative control (NC).

were not recognized. The reactivity of G8B4 was restored at Δ73–87 and Δ85–99 N. Evaluation of these deleted constructs of MTNV N protein in Western blotting using mAb E5G6 showed comparable levels of expression (Fig. 2B).

Reactivity of the mAbs to MTNV N proline-36 (Pro36) substituted with alanine by IFA, ELISA, and Western blotting

To assess the role of the N-terminal coiled-coil α-helix conformation in mAb reactivity, Pro36 in the full-length N protein was replaced with alanine (P36A). When examined by IFA in transfected cells, all of the mAbs reacted with the P36A mutant; compared with wild type, the intensity varied but was weaker overall, especially for mAb 2H10 (data not shown). A similar pattern was observed on capture ELISA and Western blotting using a 293T cell antigen lysate (Fig. 3A and B). Differential expression of the wild-type and P36A mutant proteins as the cause of the disparity was assessed using mAb E5G6, which had an epitope located outside the N-terminal domain that showed equal band sizes on Western blotting, suggesting comparable levels of expression of the two constructs (Fig. 3C).

Mapping of the topological relationships by a competitive binding assay

We performed a competitive binding capture ELISA to determine the topological relationships of the epitopes within the N-terminus using full-length MTNV N protein (Fig. 4). The assay

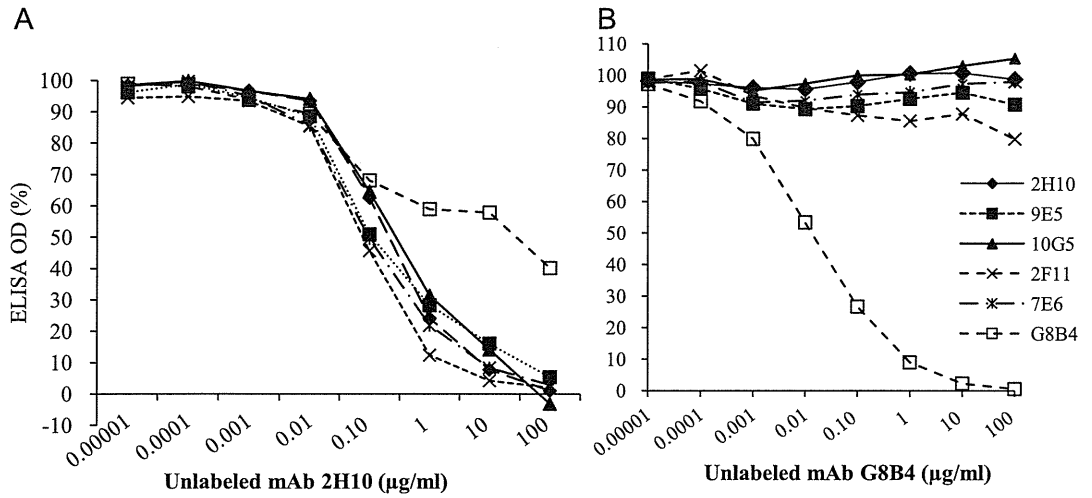

Fig. 4. Competitive ELISA of the six mAbs showing the inhibition of biotin-labeled mAbs on MTNV N protein using 10-fold serial dilutions of unlabeled mAbs. (A) Example of the complete inhibition pattern of mAb 2H10 to the other four mAbs (9E5, 10G5, 7E6, and 2F11), except for G8B4, which exhibited partial inhibition. (B) Reverse set up of G8B4 competitor (unlabeled) showing the complete inhibition to homologous labeled G8B4 and the absence of inhibition of the other five mAbs.

identified two prominent and partially overlapping regions. Five mAbs (2H10, 9E5, 10G5, 2F11, and 7E6) showed complete two-way inhibition, and, as anticipated, G8B4 showed partial inhibition (50–60%) when the five other mAbs were used as competitors (Fig. 4A). However, when the format was reversed (i.e., with G8B4 as the competitor [unlabeled]), no inhibition was observed in the other five mAbs (Fig. 4B), consistent with our deleted mutant epitope mapping results that showed partial overlap between G8B4 and the other mAbs (Table 5).

Discussion

The generation of mAbs for detecting hantaviruses is an important approach to obtain information on the antigenic properties of hantaviruses, especially in Mexico, because few hantavirus-related studies have been conducted so far. In this study, we generated and characterized six mAbs directed against the MTNV N protein that had extended cross-reactivity to a wide range of rodent-borne hantavirus N proteins expressed in bacteria, baculovirus, and mammalian systems. The region of the N protein responsible for eliciting this strong cross-reactivity was mapped to discontinuous epitopes within the N-terminus.

As is common with hantaviruses, we observed that all of the mAbs targeted the N-terminus, a region known to be immunodominant. A preliminary assessment of mAb reactivity on ELISA indicated a relatively wide spectrum of cross-reactivity to other hantavirus antigens. Additionally, we observed that all of the mAbs recognized SDS-treated antigens on Western blotting (Fig. 1B). Because the MTNV N protein used for mouse immunization was expressed in *Escherichia coli*, our initial concern was that these cross-reactive antigenic determinants could be bacteria-specific and absent from other systems or authentic virus N protein. Thus, we examined the reactivity of the mAbs to hantavirus N proteins expressed in other systems.

Although a comprehensive comparison of the antigens could not be made between the bacterial and baculovirus expression systems, the results of the five mAbs (2H10, 9E5, 10G5, 2F11, and 7E6) were consistent. While G8B4 reactivity was restricted mainly to the North American hantaviruses, in bacterial expression, G8B4 reacted with MTNV, CARV, HUIV, and SNV but in baculovirus expression, only homologous MTNV was positive. The reason why the reactivity of G8B4 was lost in baculovirus system is not clear. It is likely that the bacterial expression and other expression systems preserve the epitope conformation. Moreover, mAb 7E6 recognized all of the European and Asian hantaviruses examined, at least to some degree. Furthermore, these differences appeared to have a greater effect on the ability of the mAbs to react with heterologous antigens, such as the European and Asian viruses. As noted, when mAb reactivity to native N protein was examined in mammalian cells by IFA, four mAbs strongly recognized antigens of all the hantaviruses considered (Table 3). This recognition of N protein in virus-infected cells confirmed that the epitopes eliciting the cross-reactive B-cell response to bacterially-expressed antigen were authentic. Additionally, the failure of the mAbs to recognize authentic TPMV antigen showed that the target epitopes may assume a different conformation in Soricomorpha-borne hantavirus N protein or be absent altogether (Yadav et al., 2007).

The reactivity to truncated MTNV N fragments highlights the immunodominant nature of the protein's N-terminus (Elgh et al., 1996; Lundkvist et al., 1996). Moreover, the failure to react with the fragment N46–125 is worth noting because it suggests the need for the complete stretch of N-terminal residues. These results are consistent with previous findings showing that the first 100 aas comprise the immunodominant region of hantavirus N protein (Geldmacher et al., 2004; Gott et al., 1997). Further examination of mAb reactivity using N-terminus-deleted mutants shed more light on the binding properties. We found that those mAbs with the highest level of cross-reactivity (2H10, 9E5, 2F11, 10G5 and 7E6) bound to residues 13–51, a region previously shown to induce a cross-reactive immune response in hantavirus-infected humans (Jenison et al., 1994). Our initial speculation was that the mAbs were targeting linear epitopes because they recognized SDS-treated antigens strongly on Western blotting. However, an evaluation of reactivity using the deleted mutants suggested that the mAbs could be targeting non-linear or conformational epitopes (Table 5).

To further explore this observation, given that the N-terminus forms a coiled-coil α-helix conformation, we hypothesized that if attachment of the mAbs involved straddling between the N protein helices, substituting the residue Pro36 would interfere with reactivity. A previous study demonstrated that the substitution of Pro36 destabilized the coiled–coiled conformation but

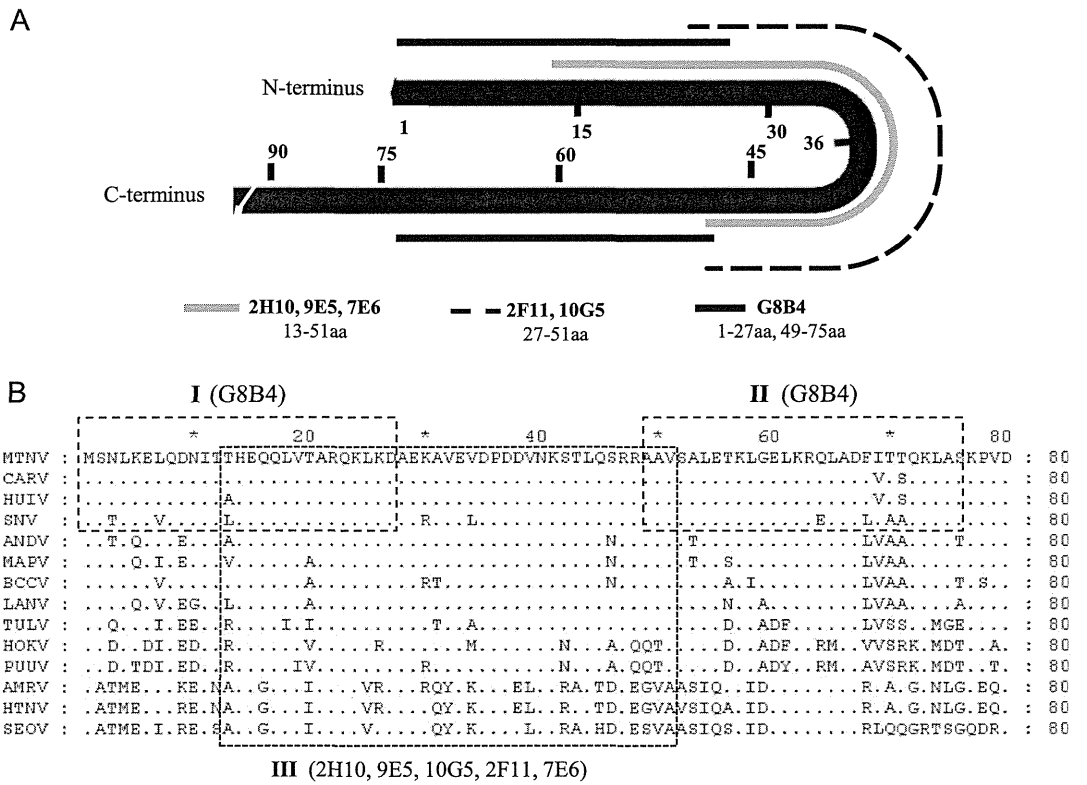

Fig. 5. Binding regions of the mAbs, as determined using truncated and deleted N protein mutants. (A) Schematic view of the residues (aas 1–100) at the MTNV N protein N-terminus recognized by the six mAbs. The mAb and residues necessary for reactivity included: G8B4, (aas 1–27 and 49–75) open bar; 2H10, 9E5, and 7E6 (aas 13–51), gray bar; and 2F11 and 10G5 (aas 25–51), broken lines. (B) Alignment of the N-terminal residues (aas 1–80) from the hantaviruses used in the analysis, showing the binding regions of G8B4 (I and II) and 2H10, 9E5, 10G5, 2F11, and 7E6 (III).

preserved the secondary α-helix structure (Wang et al., 2008). For this experiment, Pro36 was substituted with alanine to uncouple the helix–helix interaction, while, as much as possible, maintaining the secondary structure of the helix. The reactivity of the mAbs to the mutant was lower than that to wild type, suggesting that the substitution destabilized the conformation of the N-terminal domain. Although we changed a single residue, Lindkvist et al. (2008) found that by substituting four residues (aas 34–38) instead, nephropathia epidemica patient polyclonal sera reactivity to a heterologous antigen was significantly affected. This indicates that these residues are involved in inducing cross-reactivity, directly as part of the epitope or indirectly, by conferring conformational stability to the protein.

A competitive ELISA confirmed that five of the six mAbs recognized similar regions. A comparison of the specific reactivity of G8B4 (aas 1–27 and 49–75) to the five other mAbs suggested the presence of broadly cross-reactive conformation-dependent epitopes within aas 13–51 at the N-terminus (Fig. 5A).

Although the exact nature of the effect of the deletions remains undetermined, the complete loss of reactivity of the mAbs to the mutant N protein due to deletions between aas 13 and 51 at the N-terminus suggests that conformational integrity of this region is necessary for antibody recognition. The residues necessary for cross-reactivity could not be defined due to the sequence diversity across the hantaviruses examined (Fig. 5B). Therefore, these cross-reactive mAbs may be useful probes for structure–function relationship studies.

In this study, we showed that within the N-terminus there are conformation-dependent epitopes responsible for inducing extensive cross-reactivity within rodent-borne hantaviruses. These data suggest that although the primary structure of the hantavirus N protein may vary, there are highly conserved antigenic determinants apparently common to rodent-borne hantaviruses, thus pointing to similar structure and function mechanisms.

Methods

Cloning of the full-length genes and truncated and deleted mutants

For the expression of full-length N protein in *E. coli* (strain AD494 pLysS), cDNAs for the entire N protein open reading frame from MTNV, CARV, and HUIV (Kariwa et al., 2012) and SNV, kindly supplied by Dr. C. J. Peters (University of Texas Medical Branch, Galveston, TX, USA), BCCV (Rollin et al., 1995), ANDV (Reynolds et al., 2007), LANV (Johnson et al., 1997), MAPV (Fulhorst et al., 2004), HTNV strain 76–118 (Lee et al., 1982), AMRV (Lokugamage et al., 2004), SEOV (Kitamura et al., 1983), PUUV strain Sotkamo (Vapalahti et al., 1992), HOKV (Kariwa et al., 1995), TULV (Tegshduuren et al., 2010) and TPMV (Carey et al., 1971) were cloned into pET43.1b(+) (Novagen) for expression as NuSA-tagged proteins. The MTNV deletion mutants were similarly prepared (Fig. 1A). Truncated MTNV N protein cDNAs encoding N1–80, N1–150, N46–125, N125–275, and N250–428 were cloned into pET32.1b (Novagen) for expression as thioredoxin (TrxA) fusion proteins (Fig. 1A). For the expression of N protein in mammalian (Vero E6 and 293T) cells, cDNAs encoding full-length or deleted MTNV N protein were cloned into the expression vector pCAGGS/MCS (Niwa et al., 1991).

For baculovirus expression, MTNV, CARV, HUIV, SNV 77734 (Botten et al., 2000), BCCV, ANDV, LANV strain 510B, and MAPV, HTNV, SEOV, PUUV, TULV, TPMV genes encoding full-length N protein were cloned into pFastBac1 (Invitrogen) and expressed in High Five cells, as described previously (Koma et al., 2010).

Preparation of recombinant N protein in bacteria

N protein was expressed as a fusion with NuSA or TrxA in *E. coli* (strain AD494 pLysS) (Fig. 1). Briefly, transformed cells were grown in Luria-Bertani medium containing 100 μg/mL ampicillin to an optical density of $A_{600}=0.6$, and expression was induced for 4 h with isopropyl-β-D-thiogalacto-pyranoside to a final concentration of 0.5 mM. The cells were recovered by centrifugation (6000*g*, 10 min), followed by His-tag affinity purification using ProBond Nickel-chelating resin (Invitrogen) and collection with Elute Buffer (50 mM Tris, pH 8.0, 0.5 M NaCl, and 250 mM imidazole) followed by desalting on PD-10 columns (GE Healthcare, Little Chalfont, Buckinghamshire, UK). The recombinant N proteins were subjected to SDS-PAGE and Western blotting with the hantavirus N-specific mAb E5G6 (Yoshimatsu et al., 1996) to verify correct expression.

Recombinant N protein expression in mammalian systems

For hantavirus N protein expression in mammalian cells, the entire open reading frame of the S segment or a series of truncated or deleted constructs encoding the desired regions were amplified and cloned into pCAGGS/MCS vector. For IFA, Vero E6 cells were seeded on 24-well slides and transfected using TransIT-LT1 transfection reagent (Mirus Bio, Madison, WI, USA). Cells infected with the following viruses were used: HTNV 76–118, SEOV SR-11, PUUV Sotkamo strain (Vapalahti et al., 1992), TULV strain Morabia, and TPMV strain VRC-66412.

The transfected or infected cells were fixed with acetone and analyzed for reactivity to the mAbs. To prepare an N protein cell lysate for ELISA and competitive binding assay, 293T cells were grown in six-well plates and transfected. Expression was carried out for 48 h. The cells were then harvested and lysed in Lysis buffer (0.01 M Tris HCl, pH 7.8, 5 mM EDTA, 0.15 M NaCl, 0.6 M KCl, and 2% Triton X-100).

Mouse immunization

Four-week-old BALB/c mice were inoculated with four doses of 0.2 mL of MTNV N-NuSA (750 μg/mL) in incomplete Freund's adjuvant (Rockland, Gilbertsville, PA, USA) at 0-, 14-, 21-, and 48-days intervals. Pre- and post-immune serum was collected and examined by ELISA for adequate specific antibody responses. Four days after the final immunization, the mice were sacrificed and their spleens harvested for the preparation of hybridomas.

All experiments involving animals in this study were approved by the Committee of Animal Experimentation of Hokkaido University.

Production of mAbs

SP2/0-Ag14 myeloma cells were mixed with the spleen cells and fused with polyethylene glycol 1500 (Roche, Indianapolis, IN, USA). The hybridomas were cultured in GIT medium (Nippon Seiyaku, Osaka, Japan) containing 2 × HAT supplement (Gibco-Invitrogen, Grand Island, USA) and BriClone (NICB, Dublin, Ireland). MTNV N antibody-secreting hybridomas were cloned at least four times by limiting dilution. ELISA was used to select hybridomas producing anti-N protein-specific antibodies using MTNV N protein and NuSA (negative control antigen). Next, eight-week-old BALB/c mice were inoculated intraperitoneally with antibody-producing hybridomas (10×10^7 cells/mouse) and ascitic fluid was collected within 2 weeks. The supernatant of the ascitic fluid was purified using an Affi-Gel Protein A MAPS II Kit (BioRad, Hercules, CA, USA) and PD-10 desalting columns. The mAb IgG subclasses were determined using IsoQuick Strips (Sigma-Aldrich, St. Louis, MO, USA) according to the manufacturer's protocol.

ELISA

ELISA microtiter plates (NUNC) were coated with recombinant N protein or NuSA-tagged protein at 2 μg/mL in carbonate-bicarbonate buffer and left at 37 °C for 1 h or 4 °C overnight. Block Ace (Dainippon Sumitomo Pharmaceutical, Osaka, Japan) was used for blocking. The plates were then incubated with hybridoma culture supernatant or purified mAbs. After washing, 1:4000-diluted peroxidase-conjugated anti-mouse IgG (Jackson ImmunoResearch, West Grove, PA, USA) was added to the plate (50 μL/well). *o*-phenylenediamine (Sigma-Aldrich) substrate was applied to the plate (100 μL/well) and left at room temperature for 30 min. The optical densities were measured at 450–650 nm using a Labsystem Multiscan MS (Helsinki, Finland). The specific reaction was calculated by subtracting the absorbance of the NuSA tag from the N protein value. All incubations were carried out for 1 h at 37 °C with three between-step washes using phosphate-buffered saline containing 0.05% Tween-20 (PBST).

Western blotting

For Western blotting, the N proteins were separated by SDS-PAGE then transferred to a PVDF membrane (Millipore, Cork, Ireland). Membrane blocking was performed using Block Ace. Next, dilute ascitic fluid or purified mAb (in PBST) was applied, followed by peroxidase-conjugated IgG (Jackson ImmunoResearch). Signals were detected using chemiluminescence ECL detection reagents (GE Healthcare) according to the manufacturer's protocol.

IFA

Vero E6 cells were seeded on 24-well slides and transfected with plasmid constructs encoding full-length, truncated, or deleted N proteins (Fig. 2). Fixed cells were incubated with 10-fold dilutions of purified mAbs, followed by Alexa-488-conjugated anti-mouse IgG antibody (Invitrogen).

Biotinylation and competitive binding assay

The competitive binding assay was performed by a capture ELISA using a streptavidin-biotin labeled system. Purified IgG (2 mg) was biotinylated using a Biotin-AC5-OSu Kit (Dojindo Molecular Technologies, Kumamoto, Japan) according to the manufacturer's protocol. Next, 96-well plates were coated with 2 μg/mL mAb (2H10) diluted in PBS, incubated overnight at 4 °C, and blocked with 3% BSA-PBS buffer. A MTNV N protein lysate prepared from 293T cells (1:20) was captured for 1 h, followed by the addition of a 10-fold excess of unlabeled mAb (from 0.1 mg/mL) in 0.5% BSA (in PBST). Biotin-labeled mAbs were added without washing, and then the plate was incubated with streptavidin-peroxidase (Invitrogen) for 30 min at room temperature. The colorimetric reaction was carried out followed by three washes with PBST. The absorbance values (450–650 nm) were categorized as positive ($>75\%$), intermediate (25–75%), or negative ($<25\%$) inhibition in relation to the reference sample without unlabeled/competing mAbs.

For the capture ELISA for the detection of baculovirus N protein in High five cell lysate, reactivity to mAbs detection was carried out using biotinylated mAb E5G6.

Acknowledgments

This work was supported financially by Grants-in-Aid for Scientific Research (16405034, 17255009, and 21405035) from the Japanese Ministry of Education, Culture, Sports, Science, and Technology; and by a Health and Labor Sciences Research Grant on Emerging and Re-Emerging Infectious Diseases from the Japanese Ministry of Health, Labor, and Welfare. This work was also supported by the Global COE Program for Zoonosis Control (Hokkaido University).

Appendix A. Supporting information

Supplementary data associated with this article can be found in the online version at doi:10.1016/j.virol.2012.03.001.

References

Alfadhli, A., Steel, E., Finlay, L., Bachinger, H.P., Barklis, E., 2002. Hantavirus nucleocapsid protein coiled-coil domains. J. Biol. Chem. 277 (30), 27103–27108.

Alminaite, A., Halttunen, V., Kumar, V., Vaheri, A., Holm, L., Plyusnin, A., 2006. Oligomerization of hantavirus nucleocapsid protein: Analysis of the N-terminal coiled-coil domain. J. Virol. 80 (18), 9073–9081.

Avsic-Zupanc, T., Xiao, S.Y., Stojanovic, R., Gligic, A., van der Groen, G., LeDuc, J.W., 1992. Characterization of Dobrava virus: A Hantavirus from Slovenia, Yugoslavia. J. Med. Virol. 38 (2), 132–137.

Bharadwaj, M., Nofchissey, R., Goade, D., Koster, F., Hjelle, B., 2000. Humoral immune responses in the hantavirus cardiopulmonary syndrome. J. Infect. Dis. 182 (1), 43–48.

Botten, J., Mirowsky, K., Kusewitt, D., Bharadwaj, M., Yee, J., Ricci, R., Feddersen, R.M., Hjelle, B., 2000. Experimental infection model for Sin Nombre hantavirus in the deer mouse (*Peromyscus maniculatus*). Proc. Natl. Acad. Sci. USA 97 (19), 10578–10583.

Boudko, S.P., Kuhn, R.J., Rossmann, M.G., 2007. The coiled-coil domain structure of the Sin Nombre virus nucleocapsid protein. J. Mol. Biol. 366 (5), 1538–1544.

Carey, D.E., Reuben, R., Panicker, K.N., Shope, R.E., Myers, R.M., 1971. Thottapalayam virus: A presumptive arbovirus isolated from a shrew in India. Indian J. Med. Res. 59 (11), 1758–1760.

Cheng, E., Haque, A., Rimmer, M.A., Hussein, I.T., Sheema, S., Little, A., Mir, M.A., 2011. Characterization of the interaction between hantavirus nucleocapsid protein (N) and ribosomal protein S19 (RPS19). J. Biol. Chem. 286 (13), 11814–11824.

Chu, Y.-K., Owen, R.D., Sanchez-Hernandez, C., Romero-Almaraz, M. d.L., Jonsson, C.B., 2008. Genetic characterization and phylogeny of a hantavirus from Western Mexico. Virus Res. 131 (2), 180–188.

de Carvalho Nicacio, C., Gonzalez Della Valle, M., Padula, P., Bjorling, E., Plyusnin, A., Lundkvist, A., 2002. Cross-protection against challenge with Puumala virus after immunization with nucleocapsid proteins from different hantaviruses. J. Virol. 76 (13), 6669–6677.

Elgh, F., Lundkvist, A., Alexeyev, O.A., Wadell, G., Juto, P., 1996. A major antigenic domain for the human humoral response to Puumala virus nucleocapsid protein is located at the amino-terminus. J. Virol. Methods 59 (1-2), 161–172.

Fulhorst, C.F., Cajimat, M.N., Utrera, A., Milazzo, M.L., Duno, G.M., 2004. Maporal virus, a hantavirus associated with the fulvous pygmy rice rat (*Oligoryzomys fulvescens*) in western Venezuela. Virus Res. 104 (2), 139–144.

Geldmacher, A., Skrastina, D., Petrovskis, I., Borisova, G., Berriman, J.A., Roseman, A.M., Crowther, R.A., Fischer, J., Musema, S., Gelderblom, H.R., Lundkvist, A., Renhofa, R., Ose, V., Kruger, D.H., Pumpens, P., Ulrich, R., 2004. An amino-terminal segment of hantavirus nucleocapsid protein presented on hepatitis B virus core particles induces a strong and highly cross-reactive antibody response in mice. Virology 323 (1), 108–119.

Gott, P., Zoller, L., Darai, G., Bautz, E.K., 1997. A major antigenic domain of hantaviruses is located on the aminoproximal site of the viral nucleocapsid protein. Virus Genes 14 (1), 31–40.

Hjelle, B., Jenison, S., Torrez-Martinez, N., Yamada, T., Nolte, K., Zumwalt, R., MacInnes, K., Myers, G., 1994. A novel hantavirus associated with an outbreak of fatal respiratory disease in the southwestern United States: evolutionary relationships to known hantaviruses. J. Virol. 68 (2), 592–596.

Jenison, S., Yamada, T., Morris, C., Anderson, B., Torrez-Martinez, N., Keller, N., Hjelle, B., 1994. Characterization of human antibody responses to four corners hantavirus infections among patients with hantavirus pulmonary syndrome. J. Virol. 68 (5), 3000–3006.

Johnson, A.M., Bowen, M.D., Ksiazek, T.G., Williams, R.J., Bryan, R.T., Mills, J.N., Peters, C.J., Nichol, S.T., 1997. Laguna Negra virus associated with HPS in western Paraguay and Bolivia. Virology 238 (1), 115–127.

Jonsson, C.B., Figueiredo, L.T., Vapalahti, O., 2010. A global perspective on hantavirus ecology, epidemiology, and disease. Clin. Microbiol. Rev. 23 (2), 412–441.

Kariwa, H., Yoshida, H., Sánchez-Hernández, C., Romero-Almaraz, M. a. d.L., Almaraz- Catalán, J.A., Ramos, C., Miyashita, D., Seto, T., Takano, A., Totani, M., Murata, R., Saasa, N., Ishizuka, M., Sanada, T., Yoshii, K., Yoshimatsu, K., Arikawa, J., Takashima, I., 2012. Genetic diversity of hantaviruses in Mexico: Identification of three novel hantaviruses from Neotominae rodents. Virus Res. 163 (2), 486–494.

Kariwa, H., Yoshizumi, S., Arikawa, J., Yoshimatsu, K., Takahashi, K., Takashima, I., Hashimoto, N., 1995. Evidence for the existence of Puumula-related virus among *Clethrionomys rufocanus* in Hokkaido, Japan. Am. J. Trop. Med. Hyg. 53 (3), 222–227.

Kaukinen, P., Koistinen, V., Vapalahti, O., Vaheri, A., Plyusnin, A., 2001. Interaction between molecules of hantavirus nucleocapsid protein. J. Gen. Virol. 82 (Pt 8), 1845–1853.

Kitamura, T., Morita, C., Komatsu, T., Sugiyama, K., Arikawa, J., Shiga, S., Takeda, H., Akao, Y., Imaizumi, K., Oya, A., Hashimoto, N., Urasawa, S., 1983. Isolation of virus causing hemorrhagic fever with renal syndrome (HFRS) through a cell culture system. Jpn. J. Med. Sci. Biol. 36 (1), 17–25.

Koma, T., Yoshimatsu, K., Pini, N., Safronetz, D., Taruishi, M., Levis, S., Endo, R., Shimizu, K., Yasuda, S.P., Ebihara, H., Feldmann, H., Enria, D., Arikawa, J., 2010. Truncated hantavirus nucleocapsid proteins for serotyping Sin Nombre, Andes, and Laguna Negra hantavirus infections in humans and rodents. J. Clin. Microbiol. 48 (5), 1635–1642.

Kucinskaite-Kodze, I., Petraityte-Burneikiene, R., Zvirbliene, A., Hjelle, B., Medina, R.A., Gedvilaite, A., Razanskiene, A., Schmidt-Chanasit, J., Mertens, M., Padula, P., Sasnauskas, K., Ulrich, R.G., 2011. Characterization of monoclonal antibodies against hantavirus nucleocapsid protein and their use for immunohistochemistry on rodent and human samples. Arch. Virol. 156 (3), 443–456.

Lee, H.W., Baek, L.J., Johnson, K.M., 1982. Isolation of Hantaan virus, the etiologic agent of Korean hemorrhagic fever, from wild urban rats. J. Infect. Dis. 146 (5), 638–644.

Li, G., Pan, L., Mou, D., Chen, Y., Zhang, Y., Li, X., Ren, J., Wang, P., Jia, Z., Huang, C., Sun, Y., Yang, W., Xiao, S.Y., Bai, X., 2006. Characterization of truncated hantavirus nucleocapsid proteins and their application for serotyping. J. Med. Virol. 78 (7), 926–932.

Lindkvist, M., Lahti, K., Lilliehook, B., Holmstrom, A., Ahlm, C., Bucht, G., 2007. Cross-reactive immune responses in mice after genetic vaccination with cDNA encoding hantavirus nucleocapsid proteins. Vaccine 25 (9), 1690–1699.

Lindkvist, M., Naslund, J., Ahlm, C., Bucht, G., 2008. Cross-reactive and serospecific epitopes of nucleocapsid proteins of three hantaviruses: Prospects for new diagnostic tools. Virus Res. 137 (1), 97–105.

Lokugamage, K., Kariwa, H., Lokugamage, N., Miyamoto, H., Iwasa, M., Hagiya, T., Araki, K., Tachi, A., Mizutani, T., Yoshimatsu, K., Arikawa, J., Takashima, I., 2004. Genetic and antigenic characterization of the Amur virus associated with hemorrhagic fever with renal syndrome. Virus Res. 101 (2), 127–134.

Lundkvist, A., Kallio-Kokko, H., Sjolander, K.B., Lankinen, H., Niklasson, B., Vaheri, A., Vapalahti, O., 1996. Characterization of Puumala virus nucleocapsid protein: Identification of B-cell epitopes and domains involved in protective immunity. Virology 216 (2), 397–406.

Martinez, V.P., Bellomo, C., San Juan, J., Pinna, D., Forlenza, R., Elder, M., Padula, P.J., 2005. Person-to-person transmission of Andes virus. Emerg. Infect. Dis. 11 (12), 1848–1853.

Morii, M., Yoshimatsu, K., Arikawa, J., Zhou, G., Kariwa, H., Takashima, I., 1998. Antigenic characterization of Hantaan and Seoul virus nucleocapsid proteins expressed by recombinant baculovirus: Application of a truncated protein, lacking an antigenic region common to the two viruses, as a serotyping antigen. J. Clin. Microbiol. 36 (9), 2514–2521.

Niwa, H., Yamamura, K., Miyazaki, J., 1991. Efficient selection for high-expression transfectants with a novel eukaryotic vector. Gene 108 (2), 193–199.

Okumura, M., Yoshimatsu, K., Kumperasart, S., Nakamura, I., Ogino, M., Taruishi, M., Sungdee, A., Pattamadilok, S., Ibrahim, I.N., Erlina, S., Agui, T., Yanagihara, R., Arikawa, J., 2007. Development of serological assays for Thottapalayam virus, an insectivore-borne Hantavirus. Clin. Vaccine Immunol. 14 (2), 173–181.

Reynolds, S., Galanis, E., Krajden, M., Morshed, M., Bowering, D., Abelson, W., Kollmann, T.R., 2007. Imported fatal hantavirus pulmonary syndrome. Emerg. Infect. Dis. 13 (9), 1424–1425.

Rollin, P.E., Ksiazek, T.G., Elliott, L.H., Ravkov, E.V., Martin, M.L., Morzunov, S., Livingstone, W., Monroe, M., Glass, G., Ruo, S., et al., 1995. Isolation of black creek canal virus, a new hantavirus from Sigmodon hispidus in Florida. J. Med. Virol. 46 (1), 35–39.

Schmaljohn, C.S., Jennings, G.B., Hay, J., Dalrymple, J.M., 1986. Coding strategy of the S genome segment of Hantaan virus. Virology 155 (2), 633–643.

Severson, W., Xu, X., Kuhn, M., Senutovitch, N., Thokala, M., Ferron, F., Longhi, S., Canard, B., Jonsson, C.B., 2005. Essential amino acids of the hantaan virus N protein in its interaction with RNA. J. Virol. 79 (15), 10032–10039.

Severson, W.E., Xu, X., Jonsson, C.B., 2001. cis-Acting signals in encapsidation of Hantaan virus S-segment viral genomic RNA by its N protein. J. Virol. 75 (6), 2646–2652.

Tegshduuren, E., Yoshimatsu, K., Taruishi, M., Endo, R., Shimizu, K., Koma, T., Yasuda, S.P., Kariwa, H., Arikawa, J., Ishihara, C., 2010. Different cross-reactivity

of human and rodent sera to Tula virus and Puumala virus. Comp. Immunol. Microbiol. Infect. Dis. 33 (6), e67–e73.
Tischler, N.D., Rosemblatt, M., Valenzuela, P.D., 2008. Characterization of cross-reactive and serotype-specific epitopes on the nucleocapsid proteins of hantaviruses. Virus Res. 135 (1), 1–9.
Torrez-Martinez, N., Song, W., Hjelle, B., 1995. Nucleotide sequence analysis of the M genomic segment of El Moro Canyon hantavirus: Antigenic distinction from four corners hantavirus. Virology 211 (1), 336–338.
Vapalahti, O., Kallio-Kokko, H., Salonen, E.M., Brummer-Korvenkontio, M., Vaheri, A., 1992. Cloning and sequencing of Puumala virus Sotkamo strain S and M RNA segments: Evidence for strain variation in hantaviruses and expression of the nucleocapsid protein. J. Gen. Virol. 73 (4), 829–838.
Wang, Y., Boudreaux, D.M., Estrada, D.F., Egan St., C.W., Jeor, S.C., De Guzman, R.N., 2008. NMR structure of the N-terminal coiled coil domain of the Andes hantavirus nucleocapsid protein. J. Biol. Chem. 283 (42), 28297–28304.
Xu, X., Severson, W., Villegas, N., Schmaljohn, C.S., Jonsson, C.B., 2002. The RNA binding domain of the hantaan virus N protein maps to a central, conserved region. J. Virol. 76 (7), 3301–3308.
Yadav, P.D., Vincent, M.J., Nichol, S.T., 2007. Thottapalayam virus is genetically distant to the rodent-borne hantaviruses, consistent with its isolation from the Asian house shrew (*Suncus murinus*). Virol. J. 4, 80.
Yoshimatsu, K., Arikawa, J., Tamura, M., Yoshida, R., Lundkvist, A., Niklasson, B., Kariwa, H., Azuma, I., 1996. Characterization of the nucleocapsid protein of Hantaan virus strain 76-118 using monoclonal antibodies. J. Gen. Virol. 77 (4), 695–704.

Journal of General Virology (2012), **93**, 27–38 DOI 10.1099/vir.0.035964-0

A conserved region in the prM protein is a critical determinant in the assembly of flavivirus particles

Kentaro Yoshii,[1] Manabu Igarashi,[2] Osamu Ichii,[3] Kana Yokozawa,[1] Kimihito Ito,[2] Hiroaki Kariwa[1] and Ikuo Takashima[1]

[1]Laboratory of Public Health, Graduate School of Veterinary Medicine, Hokkaido University, Kita-18 Nishi-9, Kita-ku, Sapporo, Hokkaido 060-0818, Japan

[2]Department of Bioinformatics, Research Center for Zoonosis Control, Hokkaido University, Kita-18 Nishi-9, Kita-ku, Sapporo, Hokkaido 060-0818, Japan

[3]Laboratory of Anatomy, Graduate School of Veterinary Medicine, Hokkaido University, Kita-18 Nishi-9, Kita-ku, Sapporo, Hokkaido 060-0818, Japan

Correspondence
Kentaro Yoshii
kyoshii@vetmed.hokudai.ac.jp

Received 3 July 2011
Accepted 21 September 2011

Flaviviruses are assembled to bud into the lumen of the endoplasmic reticulum (ER) and are secreted through the vesicle transport pathway, but the details of the molecular mechanism of virion assembly remain largely unknown. In this study, a highly conserved region in the prM protein was identified among flaviviruses. In the subviral particle (SP) system of tick-borne encephalitis virus (TBEV) and Japanese encephalitis virus, secretion of SPs was impaired by a mutation in the conserved region in the prM protein. Viral proteins were sparse in the Golgi complex and accumulated in the ER. Ultrastructural analysis revealed that long filamentous structures, rather than spherical SPs, were observed in the lumen of the ER as a result of the mutation. The production of infectious virions derived from infectious cDNA of TBEV was also reduced by mutations in the conserved region. Molecular modelling analysis suggested that the conserved region is important for the association of prM–envelope protein heterodimers in the formation of a spike of immature virion. These results are the first demonstration that the conserved region in the prM protein is a molecular determinant for the flavivirus assembly process.

INTRODUCTION

Enveloped viruses bud through cellular membranes, such as the plasma membrane, the membrane of the endoplasmic reticulum (ER) and the Golgi complex. Flaviviruses are generally thought to bud into the ER of virus-infected cells (Lindenbach *et al.*, 2007). Individual particles are subsequently transported to the Golgi complex in transport vesicle and released by exocytosis via the *trans*-Golgi network (Mackenzie & Westaway, 2001). However, intermediate budding structures have not been observed and the details of the mechanism of assembly and secretion are still largely unknown.

Flaviviruses, belonging to the family *Flaviviridae*, include many clinically important human pathogens, such as dengue (1–4) serotype viruses, West Nile virus, Japanese encephalitis virus (JEV), yellow fever virus and tick-borne encephalitis virus (TBEV) (Lindenbach *et al.*, 2007). The flavivirus genome consists of a positive-polarity ssRNA of approximately 11 kb, which encodes three structural proteins: the core (C), pre-membrane (prM)/membrane (M) and envelope (E) proteins. It also encodes seven non-structural (NS) proteins: NS1, NS2A, NS2B, NS3, NS4A, NS4B and NS5, within a single long ORF (Chambers *et al.*, 1990). The ORF is translated into a large polyprotein, which is co- or post-translationally cleaved by cellular and viral proteases.

Flavivirus virions are 40–50 nm in diameter, spherical in shape and contain a nucleocapsid and an envelope. The envelope has two viral proteins: the major envelope protein E and the small membrane protein prM/M. Cryo-electron microscopy analysis of the immature dengue virus revealed 60 spikes, each comprising three prM/E heterodimers, that are organized icosahedrally on the surface of the particles (Zhang *et al.*, 2003), in contrast to the smooth surface of mature virions reported previously (Kuhn *et al.*, 2002).

The M protein is synthesized as a precursor protein, prM, in the ER and contains one to three *N*-linked glycosylation sites (Chambers *et al.*, 1990). Newly synthesized E and prM proteins associate to form heterodimers that are incorporated into immature virions (Allison *et al.*, 1995b; Wengler & Wengler, 1989). One of the major functions of the prM protein is a chaperone-like activity aiding folding and maturation of E proteins (Konishi & Mason, 1993; Lorenz *et al.*, 2002). During transport of the virions

A supplementary figure and table are available with the online version of this paper.

through the ER and Golgi complex to the cell surface, the prM proteins of the heterodimers protect the E proteins from premature fusion by the low-pH conditions in the transport vesicles (Guirakhoo *et al.*, 1991, 1992; Heinz *et al.*, 1994; Zhang *et al.*, 2003). Prior to release from the cell, the cellular furin protease cleaves the pr portion from prM, resulting in rearrangement of the E proteins into head-to-tail homodimers on the surface of the mature virus particles (Elshuber *et al.*, 2003; Stadler *et al.*, 1997). Other roles of the prM protein are not well understood.

In flaviviruses, it has been demonstrated that subviral particles (SPs) are assembled and secreted from cells expressing the viral prM and E genes (Allison *et al.*, 1995b; Fonseca *et al.*, 1994; Mason *et al.*, 1991; Op De Beeck *et al.*, 2003; Yamshchikov & Compans, 1993). These SPs are similar to the slowly sedimenting haemagglutinin particles that are released from flavivirus-infected cells in addition to infectious virions (Gritsun *et al.*, 1989; Heinz & Kunz, 1977). SPs contain viral E proteins but lack the nucleocapsid protein and viral RNA. Because the characteristics of the envelope proteins in SPs are structurally and functionally similar to those of authentic virions, SPs have been used in research of the viral E proteins (Allison *et al.*, 1995a, 1999, 2001; Lorenz *et al.*, 2003).

Despite recent advances in our understanding of flaviviruses, the functional residues of the prM ectodomain that are important for assembly and secretion of the virions remain almost unknown. In our previous study, a single point mutation in the prM protein was found to reduce the secretion of TBEV particles, suggesting that prM plays a crucial role in the virus budding process (Yoshii *et al.*, 2004). In the current study, a highly conserved region in the prM protein was identified among flaviviruses. Several amino acid substitutions were introduced into this conserved region by site-directed mutagenesis in the SP systems of TBEV and JEV to examine their effects on the assembly and secretion of SPs. Some of these mutations were then introduced into an infectious cDNA clone of TBEV to confirm the role of the conserved region in the virus replication cycle.

RESULTS

Effect of point mutations in the conserved region of prM proteins on SP secretion

From a multiple-sequence analysis of the flavivirus prM protein, a highly conserved region was identified among flaviviruses (analysis of >4000 strains using Pfam: http://pfam.sanger.ac.uk/; Finn *et al.*, 2010). Table 1 shows the sequence of the conserved region among representative flaviviruses. To investigate the importance of this region in virus replication, alanine substitutions were engineered in this region of the pCAG-TBEME plasmid, which expresses the prM and E proteins of TBEV (Table 2). Alanine substitutions were also engineered at cysteines 68 and 70, but no expression of viral proteins was observed in cells transfected with these plasmids (data not shown). This may have been due to a critical conformational change in the prM protein, as both cysteine residues stabilize the prM structure by disulfide bonds (Li *et al.*, 2008).

pCAG-TBEME plasmids containing the different mutations were transfected into 293T cells. After incubation for 24 h, extracellular E proteins were detected by ELISA. As presented in Fig. 1(a), the secretion of E protein was reduced considerably by prM mutations at proline-63, aspartate-65, valine-66, aspartate-67 and phenylalanine-69. An alanine substitution of glutamate-62 did not affect the kinetics of the E protein. Interestingly, the conservative valine-to-alanine substitution at residue 66 reduced the secretion of the E protein. At position 66, a branched-chain amino acid (valine, isoleucine or leucine) is conserved, and a

Table 1. A conserved sequence in flavivirus prM protein

The non-conserved amino acid in the sequence is shown in non-bold.

Virus*	GenBank accession no.	Amino acid sequence									Amino acid range†
TBEV	AB062063	E	P	V	D	V	D	C	F	C	62–70
POWV	NC_003687	E	P	V	D	V	D	C	F	C	62–70
LANV	AF253419	E	P	V	D	V	D	C	F	C	58–66
JEV	AF069076	D	P	E	D	V	D	C	W	C	61–69
WNV	AB185914	D	P	E	D	I	D	C	W	C	61–69
DENV	U87411	E	P	E	D	I	D	C	W	C	60–68
YFV	X03700	E	P	D	D	I	D	C	W	C	57–65
APOIV	NC_003676	E	P	V	D	L	D	C	F	C	57–65
Consensus		E/D	P	–	D	V/I/L	D	C	F/W	C	

*POWV, Powassan virus; LANV, Langat virus; DENV, dengue virus; YFV, yellow fever virus; APOIV, Apoi virus.
†Numbers indicate the amino acid position in the prM protein.